

**A NOVEL DEEP LEARNING FRAMEWORK FOR THE
DETECTION OF LYMPHOCYTES CANCER, AND ITS TYPES**

BY

RAHEEL BAIG

REGISTRATION # 18111719-012

MASTER OF SCIENCES

Department of Computer Science



UNIVERSITY OF GUJRAT

Session 2018 - 21

Raheel Baig

MS Computer Science

2018 - 2021

**A NOVEL DEEP LEARNING FRAMEWORK FOR THE
DETECTION OF LYMPHOCYTES CANCER, AND ITS TYPES**

**A Thesis Submitted in Partial Fulfilment of the Requirements for the
Award of Degree of**

Master of Science

In

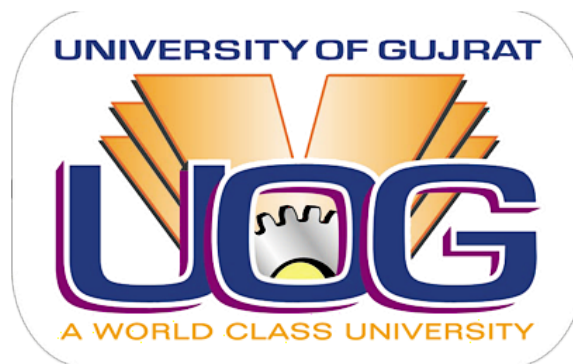
Computer Science

BY

RAHEEL BAIG

REGISTRATION # 18111719-012

Department of Computer Science



UNIVERSITY OF GUJRAT

Session 2018 - 21

ACKNOWLEDGEMENT

I am very grateful to Allah Almighty because of His love and strength that he has given to me to finish my research. I express my special thanks to my supervisor, Dr Abdur Rehman; without his assistance, direction, encouragement, suggestions, and continuous guidance, this thesis could not have been possible. The most incredible debt I owe to my parents for their constant support, and inspiration, not for this project but in all aspects of my life. I acknowledged that many people help me make this whole process successful within a limited time frame.

I would also like to thank Professor Dr Ikram Ullah Ilali for helping throughout the experimental work.

Raheel Baig

DEDICATION

I would like to dedicate my work to my parents, sisters, especially most reverenced supervisor and Professor Dr Ikram Ullah Ilali for their endless support, love, and encouragement.

Raheel Baig

DECLARATION

I, Raheel Baig S/O Mirza Faique Baig, roll no 18111719-012, MS Computer Science scholar, University of Gujrat, Pakistan, hereby solemnly declare that this thesis titled “A Novel Deep Learning Framework for The Detection of Lymphocytes Cancer, and its Types” is based on genuine work, and has not yet been submitted or published elsewhere. I shall not use this thesis for obtaining any other degree from this University or any other Institution.

I also understand that if plagiarism is found in this thesis at any stage, even after the award of the degree, the degree may be cancelled and revoked by the University.

Raheel Baig

It is certified that Mr Raheel Baig S/O Mirza Faique Baig, roll no 18111719-012, MS Computer Science Scholar, Department of Computer Science, Faculty of Computing, and IT, University of Gujrat, Pakistan, worked under my supervision. The above-stated declaration is correct to the best of my knowledge.

Dr Abdur Rehman
Assistant Professor,
University of Gujrat, Gujrat, Pakistan.
Email: a.rehman@uog.edu.pk
Dated: 1st Sep, 2021

THESIS COMPLETION CERTIFICATE

It is certified that this thesis titled “A Novel Deep Learning Framework for The Detection of Lymphocytes Cancer, and its Types” submitted by Mr Raheel Baig s/o Mirza Faique Baig, roll # 18111719-012, MS Computer Science Scholar, Department of Computer Science, Faculty of Computing and IT, University of Gujrat, Pakistan, is evaluated and accepted for the award of degree “Master of Science (MS)” in Computer Science by the following members of the Thesis/ Dissection Viva Voce Examination Committee.

The evaluation report is available in the Directorate of Advanced Studies and Research Board of the University.



Dr Muhammad Usman Ghani Khan
Professor,
University of Engineering and Technology,
Lahore, Pakistan.
Email: usman.ghani@uet.edu.pk

Dr Abdur Rehman
Assistant Professor,
Department of Computer Science,
University of Gujrat,
Gujrat, Pakistan.
Email: a.rehman@uog.edu.pk

Dr. Naveed Anwer Butt
Assistant Professor/HOD,
Department of Computer Science,
University of Gujrat,
Gujrat, Pakistan.
Email: naveed@uog.edu.pk
Dated:

TABLE OF CONTENTS	
CONTENTS	PAGE
LIST OF FIGURE	vii
LIST OF TABLES.....	viii
ABSTRACT	01
CHAPTER 01: INTRODUCTION	02
1.1 Need and Significance of Research Work.....	03
1.2 Motivation	04
1.3 Problem Statement.....	05
1.4 Research Objectives	06
1.5 Thesis Organisation	06
CHAPTER 02: LITERATURE REVIEW.....	07
2.1 Pre-processing	07
2.2 Segmentation	08
2.3 Classification	09
CHAPTER 03: PROPOSED METHODOLOGY	16
3.1 Image Acquisitions	17
3.2 Image Pre-processing	17
3.3 Data Augmentation.....	19
3.4 Image Classification	19
3.5 Feature Fusion	19
3.5.1 Convolution Neural Network Model CNN-1	19
3.5.2 Convolution Neural Network CNN-2	21
3.5.3 Feature Extraction using CNN-1 & CNN-2	22
3.5.4 Self-Convolution Neural Network Transfer Learning	22
3.6 CCA Fusion	23
3.7 Classification	23
CHAPTER 04: EXPERIMENTAL SETUP AND RESULTS	24
4.1 Dataset	24
4.2 Experimental Setup.....	24
4.3 Features Extraction Results using CNN-1	25
4.4 Features Extraction Results using CNN-2.....	27
4.5 Classification Results using CCA Fusion.....	29
4.5.1 Statistical Analysis of Bagging Ensemble on CCA Fusion.....	29
4.5.2 Statistical Analysis of Total Boost Model on CCA Fusion.....	31
4.5.3 Statistical Analysis of Fine-KNN on CCA Fusion.....	33
4.5.4 Statistical Analysis of Medium-KNN on CCA Fusion	35
4.5.5 Statistical Analysis of Coarse-KNN on CCA Fusion.....	37
4.5.6 Statistical Analysis of SVM on CCA Fusion	39
4.5.7 Statistical Analysis of LPBoost model on CCA Fusion.....	41
4.5.8: Statistical Analysis of RUSBoost on CCA Fusion.....	43
4.6 Classification Results using Serial Fusion	45
4.6.1 Statistical Analysis of SVM on Serial Fusion	45
4.6.2 Statistical Analysis on Fine KNN Serial Fusion	47
4.6.3 Statistical Analysis of Medium KNN on Serial Fusion.....	49
4.6.4 Statistical Analysis of RUSBoost on Serial Fusion.....	51
4.6.5 Statistical Analysis of TotalBoost on Serial Fusion	53
4.6.6 Statistical Analysis of LPBoost on Serial Fusion.....	55
4.6.7 Statistical Analysis of Bagging Ensembler on Serial Fusion	57
4.6.8 Statistical Analysis of Coarse KNN on Serial Fusion	59
4.7 Classification Results using PCA Fusion	61
4.7.1 Statistical Analysis of SVM on PCA Fusion.....	61
4.7.2 Statistical Analysis on Fine KNN PCA Fusion.....	63

4.7.3 Statistical Analysis of Medium KNN on PCA Fusion	65
4.7.4 Statistical Analysis of RUSBoost on PCA Fusion	67
4.7.5 Statistical Analysis of TotalBoost on PCA Fusion	69
4.7.6 Statistical Analysis of LPBoost on PCA Fusion	71
4.7.7 Statistical Analysis of Bagging Ensembler on PCA Fusion.....	73
4.7.8 Statistical Analysis of Coarse KNN on PCA Fusion.....	75
4.8 Discussion and Comparison	77
CHAPTER 05: CONCLUSION	79
REFERENCES	80
APPENDICES	83

LIST OF FIGURES	CONTENTS	PAGE
Figure-1.1: Sample image of Elements of Healthy Blood -----	02	
Figure-1.2: Sample image of Elements of Blood caused leukaemia -----	04	
Figure-3.1: Proposed Architecture -----	16	
Figure-3.2: Samples of pre-processing -----	18	
Figure-3.3: CNN-1 and CNN-2 Architecture-----	22	
Figure-4.1: Confusion Matrix of CNN-1 Feature Extraction-----	26	
Figure-4.2: Confusion Matrix of CNN-2 Feature Extraction-----	28	
Figure-4.3: Confusion Matrix of Bagging Model-----	30	
Figure-4.4: Confusion Matrix of Total Boost Model-----	32	
Figure-4.5: Confusion Matrix of F-KNN -----	34	
Figure-4.6: Confusion Matrix of Medium KNN -----	36	
Figure-4.7: Confusion Matrix of Coarse KNN -----	38	
Figure-4.8: Confusion Matrix of SVM -----	40	
Figure 4.9: Confusion Matrix of LPBoost Model-----	42	
Figure 4.10: Confusion Matrix of RUSboost-----	44	
Figure 4.11: Confusion Matrix of SVM-----	46	
Figure 4.12: Confusion Matrix of Fine KNN-----	48	
Figure 4.13: Confusion Matrix of Medium KNN-----	50	
Figure 4.14: Confusion Matrix of RUSBoost -----	52	
Figure 4.15: Confusion Matrix of Total Boost -----	54	
Figure 4.16: Confusion Matrix of LPBoost-----	56	
Figure 4.17: Confusion Matrix of Bagging Esembler -----	58	
Figure 4.18: Confusion Matrix of Coarse KNN-----	60	
Figure 4.19: Confusion Matrix of SVM-----	62	
Figure 4.20: Confusion Matrix of Fine KNN-----	64	
Figure 4.21: Confusion Matrix of Medium KNN-----	66	
Figure 4.22: Confusion Matrix of RUSBoost -----	68	
Figure 4.23: Confusion Matrix of Total Boost -----	70	
Figure 4.24: Confusion Matrix of LPBoost-----	72	
Figure 4.25: Confusion Matrix of Bagging Esembler -----	74	
Figure 4.26: Confusion Matrix of Coarse KNN-----	76	

LIST OF TABLES	
CONTENTS	PAGE
Table-1.1: Estimated deaths-----	03
Table-2.1: Literature Review -----	11
Table 3.1: Data Augmentation-----	19
Table-3.2: Layered Architecture of CNN-1-----	20
Table-3.3: Layered Architecture of CNN-2-----	21
Table 4.1: No. of samples used for classification-----	24
Table-4.2: Statistics of CNN-1 Model of Individual Classes-----	25
Table-4.3: CNN-1 Combined Statistics of All Classes-----	25
Table-4.4: Statistics of CNN-2 Model of Individual Classes-----	27
Table-4.5: CNN-2 Combined Statistics of All Classes-----	27
Table-4.6: Statistics of Bagging Model using CCA Fusion -----	29
Table-4.7: Overall Statistics of Bagging Model using CCA Fusion-----	30
Table-4.8: Statistics of Total Boost Model using CCA Fusion -----	31
Table-4.9: Overall Statistics of Total Boost Model using CCA Fusion-----	31
Table-4.10: Statistics Fine KNN using CCA Fusion -----	33
Table-4.11: Overall Statistics Fine KNN using CCA Fusion -----	33
Table-4.12: Statistics of Medium KNN using CCA Fusion -----	35
Table-4.13: Overall Statistics of Medium KNN using CCA Fusion -----	35
Table-4.14: Statistics of Coarse KNN using CCA Fusion -----	37
Table-4.15: Overall Statistics of Coarse KNN using CCA Fusion -----	37
Table-4.16: Statistics of SVM using CCA Fusion -----	39
Table-4.17: Overall Statistics of SVM using CCA Fusion -----	39
Table 4.18: Statistics of LPBoost using CCA Fusion -----	41
Table 4.19: Overall Statistics of LPBoost using CCA Fusion-----	41
Table-4.20: Statistics of RUSBoost using CCA Fusion-----	43
Table-4.21: Overall Statistics of RUSBoost using CCA Fusion-----	43
Table 4.22: Statistics of SVM using Serial Fusion -----	45
Table 4.23: Overall Statistics of SVM using Serial Fusion-----	46
Table 4.24: Statistics of Fine KNN using Serial Fusion -----	47
Table 4.25: Overall Statistics of Fine KNN using Serial Fusion-----	47
Table 4.26: Statistics of Medium KNN using Serial Fusion-----	49
Table 4.27: Overall Statistics of Medium using Serial Fusion-----	49
Table 4.28: Statistics of RUSBoost using Serial Fusion -----	51
Table 4.29: Overall Statistics of RUSBoost using Serial Fusion -----	51
Table 4.30: Statistics of TotalBoost using Serial Fusion-----	53
Table 4.31: Overall Statistics of TotalBoost using Serial Fusion-----	53
Table 4.32: Statistics of LPBoost using Serial Fusion -----	55
Table 4.33: Overall Statistics of LPBoost using Serial Fusion-----	55
Table 4.34: Statistics of BaggingEsembler using Serial Fusion -----	57
Table 4.35: Overall Statistics of Bagging Esembler using Serial Fusion-----	57
Table 4.36: Statistics of Coarse KNN using Serial Fusion -----	59
Table 4.37: Overall Statistics of Coarse KNN using Serial Fusion-----	59
Table 4.38: Statistics of SVM using PCA Fusion-----	61
Table 4.39: Overall Statistics of SVM using PCA Fusion-----	62
Table 4.40: Statistics of Fine KNN using PCA Fusion-----	63
Table 4.41: Overall Statistics of Fine KNN using PCA Fusion-----	63
Table 4.42: Statistics of Medium KNN using PCA Fusion-----	65
Table 4.43: Overall Statistics of Medium using PCA Fusion -----	65
Table 4.44: Statistics of RUSBoost using PCA Fusion -----	67
Table 4.45: Overall Statistics of RUSBoost using PCA Fusion -----	67
Table 4.46: Statistics of TotalBoost using PCA Fusion-----	69

Table 4.47: Overall Statistics of TotalBoost using PCA Fusion -----	69
Table 4.48: Statistics of LPBoost using PCA Fusion-----	71
Table 4.49: Overall Statistics of LPBoost using PCA Fusion-----	71
Table 4.50: Statistics of BaggingEsembler using PCA Fusion-----	73
Table 4.51: Overall Statistics of Bagging Esembler using PCA Fusion -----	73
Table 4.52: Statistics of Coarse KNN using PCA Fusion-----	75
Table 4.53: Overall Statistics of Coarse KNN using PCA Fusion-----	75
Table-4.54: Comparison of CCA, SBA, and PCA on ML Models -----	77
Table-4.55: Comparison of Proposed Methodology-----	78

LIST OF APPENDICES	
CONTENTS	PAGE
APPENDIX-01: Abbreviations Used in Thesis -----	83
APPENDIX-02: Turnitin Originality Report -----	84

ABSTRACT

Leukaemia is a form of blood cancer that develops when our body's bone marrow contains too many white blood cells. This condition not only affects adults but is also a prevalent form of cancer in children. Treatment for leukaemia is determined by the type and the extent to which cancer has progressed across the body. It is crucial to diagnose this condition early to get adequate care and heal. Using a convolutional neural network (CNN) model, the study provides an automatic diagnostic method for detecting acute lymphoblastic leukaemia (ALL), acute myeloid leukaemia (AML), and multiple myeloma (MM). The model detects malignant leukaemia cells using microscopic blood smear images. We gathered a dataset of about 4150 images from a public directory. Pre-processing was conducted on the dataset in our suggested technique to eliminate noise, blurriness and optimise image quality. The output images of pre-processing were already. The method works very well and does not require any image segmentation. After that, we trained two parallel CCN models, which extracts features. These extracted features are concatenated by using CCA Fused method. Lastly, fused vectors are fetched to the classifier (SVM, Bagging ensemble, total boost, RUSBoost, Fine KNN). We achieved an accuracy of 97.04% by using Bagging ensemble architecture. As a result, pathologists can find this method beneficial in accurately diagnosing.

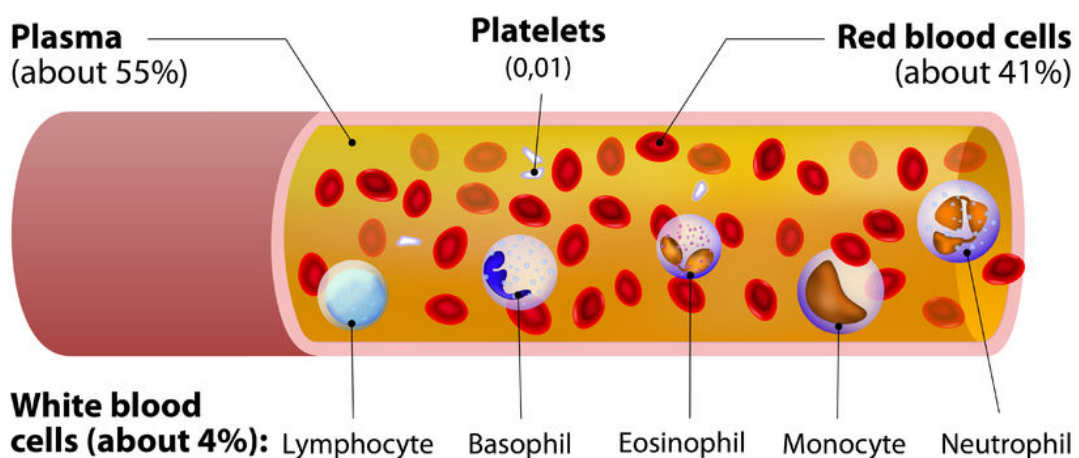
CHAPTER-01

INTRODUCTION

1: Introduction

Blood is a vital fluid that circulates in the living bodies. Blood functionality is significant among the living bodies, which carry mandatory substances to the cells, such as nutrient and oxygen. Furthermore, it also carries out the waste produced by a living organism's metabolism away from the cells (Contributors, 2019). Blood is divided into four components, that are white and red blood cells, plasma, and platelets (Subrajeet et al., n.d.).

Figure-1.1: Sample image of Elements of Healthy Blood



Source:[<http://www.alyvea.com/biologystudyguides/blood.php>]

Leukaemia is haematological cancer produced by the bone marrow, which rapidly increases the abnormal formation of **white blood cells (WBC)** in the human blood (Vogado et al., 2016). Origin of word Leukaemia comes from the Greek word "*leukos*", which means "white", and "*aim*" means "blood" (Goutam & Sailaja, 2015). Leukaemia is a fatal disease that can cause death if it is not prevented.

Leukocytes (WBC) have an essential role in the identification of various diseases. The information extracted from WBC is necessary for haematologists. To diagnose leukaemia (Vogado et al., 2018), haematologists can perform a variety of tests, and examinations, which includes blood tests, myelograms, lumbar punctures, physical examination, bone marrow biopsies, and by counting the number of white cells increased with not mature blast cells (myeloid or lymphoid), also decrease in platelets, and neutrophils (Agaian et al., 2014). Therefore, Routine examination by haematologists of the blood smears by using microscopic analysis for recognition and classification of myeloid and lymphoid cells. The overabundant existence in blast cell's bloodstream is an unusual symptom of leukaemia (Goutam & Sailaja, 2015). French American British (FAB) declared that leukaemia has

two types Chronic and Acute. These both types are further subdivided into two types: Chronic Lymphocytic Leukaemia (CLL), Chronic Myelogenous Leukaemia (CML), Acute Myelogenous Leukaemia (AML) Acute Lymphoblastic Leukaemia (ALL) respectively (Abdeldaim et al., 2018).

World Health Organization (WHO) reported the cancer mortality profile of Pakistan, which declared 1,73,937 deaths occurred due to cancer in 2018. Leukaemia is ranked 5th in Pakistan among the other cancers, 7,139 (4,264 in ale, and 2875 in females) were new cases of all sex, and the cause of leukaemia, the number of deaths was 4945 (World Health Organization, 2019).

According to the American Cancer Society, the survival, death of leukaemia varies as per the age of a person, sex, race, and p of leukaemia. The statistical analysis reported that estimated new cases were 61780 (males: 35920, females: 25860), estimated deaths were 22840 (males: 13150, females: 9690) in 2019 (Society, 2019). Estimated new cases, an estimated death of all subtypes of leukaemia is given below in the table-1. 1.

Table-1.1: Estimated deaths

Types	Cases	Deaths
Acute lymphoblastic leukemia	5,930	1,500
Acute myeloid leukaemia	21,450	10,920
Chronic myeloid leukemia	8,990	1,140
Chronic lymphocytic leukemia	20,720	3,930

Note: Estimated deaths from all types of leukaemia, 2019 (USA), American cancer society (Society, 2019).

The early detection of leukaemia cancer has a significant role in the affected person. Most commonly, 90% of affected patients of leukaemia are adults of age above 50 years, and the rest are children (Basima & Panicker, 2016). Specifically, for the children, early detection is essential for their recovery (Bhattacharjee & Saini, 2015). If cancer detection is confirmed earlier, there will be a chance to recover from the disease or prolong the patient's life.

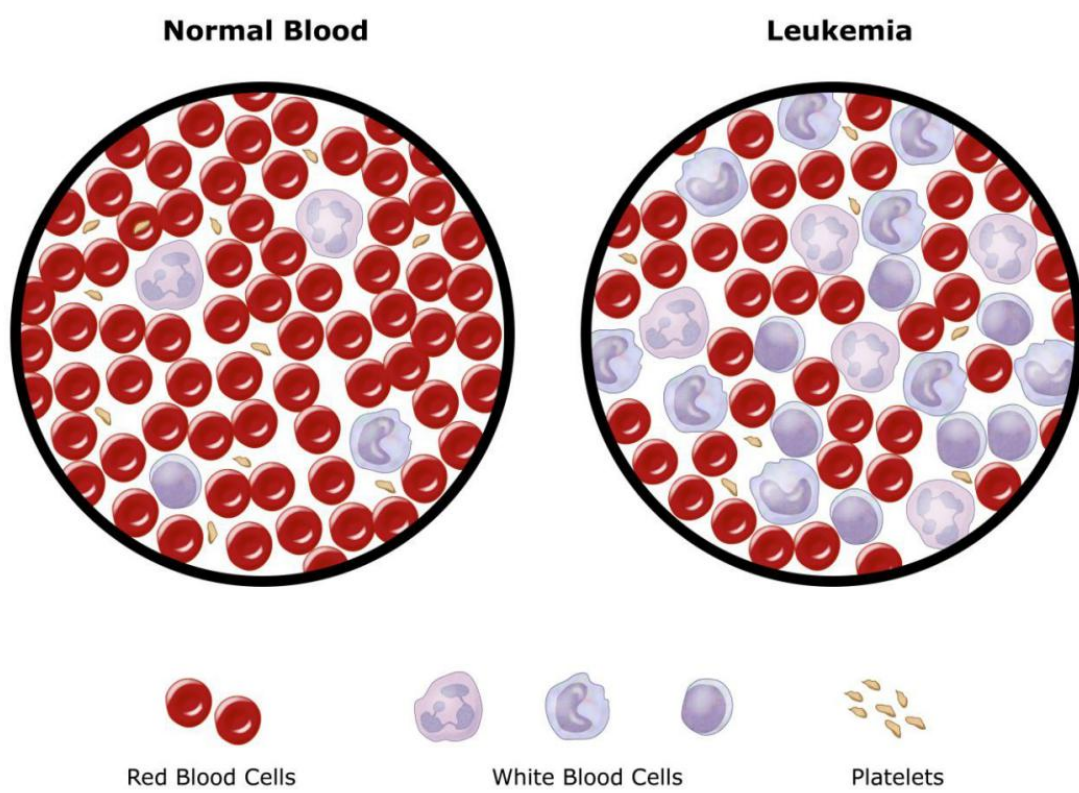
1.1: Need and Significance of Research Work

Nowadays, biomedical images play a significant part in identifying the disease, their treatments, and research in the field of health. Due to modern applications and technology, enhancement in biomedical images is censorious for analysing, diagnosing, and making clinical decisions (Chen et al., 2004). Biomedical images can detect many diseases. Similarly, leukaemia can also be detected by microscopic images of the blood. Disease development in an individual can be shown after the changes in blood cells' condition (Patel & Mishra, 2015).

It has been noted that leukaemia cancer patients are rapidly increasing, and if it is not treated at the early stages, it can lead to death. There are different methods to diagnose leukaemia with a manual and computer-aided count. The manual count's accuracy rate is reasonable when a skilled haematologist diagnoses it, but there is some drawback of this method. The most severe drawback which cannot be neglected is deadly slow analysis, non-standardised accuracy rate, and high need of the most expert haematologist (Zhao et al., 2017).

Several thousands of new patients are being diagnosed with blood cancers around the world. Due to lack of time, expert haematologist, and economy, it is difficult to diagnose the disease at an early stage or in the meantime. Hence, the computer-aided system is preferred to count the WBCs to detect the lesion. We aim to detect leukaemia at its early stage by developing a framework based on deep learning algorithms to work over microscopic images to be more persistent to cure the disease.

Figure-1.2: Sample image of Elements of Blood caused leukaemia



Source: [<https://orthoinfo.aaos.org/en/diseases--conditions/leukaemia/>]

1.2: Motivation

According to the World Health Organisation (WHO), in 2020 estimated reported cancer patients were 8350, including all ages and sex. leukaemia is ranked fifth place in Pakistan. Furthermore, statistics show that in 2025, there will be around 9300 new cases

(Organization, 2020). An increase in new cases should be encountered down to control this type of disease. This can be done by early and fast detection of disease. If it is diagnosed earlier initially, there is more chance to cure; otherwise, it may lead to death. In the past, World Health Organization (WHO) reported cancer mortality profile of Pakistan, which declared 7,139 (4,264 in males, and 2,875 in females) were new cases of all sex, and ages by the cause of leukaemia, and a total number of deaths were 4945 (World Health Organization, 2019). According to the American Cancer Society, the survival and death rate by leukaemia varies as per the age of a person, sex, race, and types of leukaemia. The statistical analysis reported that estimated new cases were 61780 (males: 35920, females: 25860), estimated deaths were 22840 (males: 13150, females: 9690) in 2019 (Society, 2019). From the statistics mentioned earlier, we can ensure the importance of early detection, which also motivates them to rehabilitate themselves from this deadly disease.

1.3: Problem Statement

Deep learning is being used widely for enhancement in medical treatments. Blood is the most crucial that flows in the living body. Death rates can be lessened if the disease is diagnosed earlier and treated in the meantime. It creates a desperate situation, and it consumes much time to detect the disease manual by the haematologist. The detection of leukaemia through computer-aided techniques is very effective, time-efficient, and much accurate to overcome these problems. Still, now, there are multiple problems, barriers, and research gaps that exist in the computer-aided system, such as the accuracy of leukaemia cancer along with its types (Acute Myelogenous Leukaemia, Acute Lymphoblastic Leukaemia, and Multiple Myeloma), and further their segmentation, and classification of their subtypes. This is a contribution to our research work.

Moreover, there are few more problems like the malignant size, the resemblance between the types of leukaemia, and between their sub-types. Noise and high resolution of test data is an issue. The availability of a small dataset is a vital problem. The use of sufficient, ad essential features have a vital role in the detection of disease. So, redundancy of features, extraction of insignificant, relevant features must be neglected as they increase the size of computation, and so, they may lead to shattering down the accuracy.

The following problems will be resolved by the proposed method:

- i. Diagnose the leukaemia cancer, types of leukaemia, further their sub-types.
- ii. Noise will be removed from training and testing microscopic images of blood.
- iii. Feature extraction of insignificant and unessential features.
- iv. Classification will be done on sample images to classify them into malignant and non-malignant classes.
- v. Classified malignant classes will also be further classified into their subtypes.

1.4: Research Objectives

- a. To propose a hybrid computer-aided diagnostic framework using deep learning that automates the cancerous region's classification from the given microscopic images.
- b. To improve the accuracy to detect cancer and lower the rate of error.
- c. To improve the execution time of detection by the haematologist.

1.5: Thesis Organisation

The remaining chapters of this booklet enclose the content as:

In the first chapter, we discussed blood and its components. Furthermore, we discussed medical imaging and how it helps us examine the internal human system; its most minor components are. As this is the introductory chapter of our research, herein, we used basic information of blood, and its components, what is leukaemia, and its types, what was the motivation to lead the topic as mentioned above, what is problem statement, which is being required to address, and at last what are our research objectives which need to be accounted. In chapter second, we discussed literature review on leukaemia. In this chapter, we consider the past work of researchers related to our research. Furthermore, in this chapter we also discussed in detail about their methodology. Past methodology includes the following steps most commonly namely pre-processing, segmentation and classification.

In next chapter 3, we explained our proposed methodology, which helps us in this search work. In this chapter we discussed image acquisitions, pre-processing, data augmentation and image classification.

In our last chapter, we explained the statistics of the results that are gathered in this research paper. After training our model by two custom build CNN models. Thereafter, we concatenated features using CCA, Serial and PCA fusion and applied classic machine learning classifiers to the fusion techniques.

CHAPTER-02

LITERATURE REVIEW

2: Literature Review

A few decades ago, computer-aided diagnostic systems and bio-medical images played an essential role in detecting various diseases. There are several techniques of segmentation and classification in the domain of machine learning and digital image processing. These techniques have played a significant role in biomedical imaging, agriculture, and video surveillance, etc.

2.1: Pre-processing

Pre-processing is a **crucial** phase that helps us enhance the visuals of medical imaging, and several techniques exist for pre-processing to make the image noiseless, clean, and enhance the quality of images.

Pre-processing is an essential phase in the field of medical image processing. Numerous techniques may apply to the images to enhance the quality of data imaging, making the image noiseless, cleaning, and enhancing the overall quality of the cytoplasm.

An author (Anwar & Alam, 2020) has adjusted rotation (rotated images from the centre between 0 degrees to 360 degrees; for data augmentation, they shifted degrees to 12 degrees), brightness, contrast, shearing, horizontal and vertical flip, and translation on images to enhance the quality of the image.

One another author (Bodzas et al., 2020) introduced their pre-processing method, which is based on arithmetic operations to remove the artistry and image enhancement. After that, gamma correction, contrast-enhancing techniques are applied. Their colour transformation is cited below by an equation.

$$g(x,y) = [(L-1)-B] - \{[(L-1)-G] \times 1/2\}$$

$g(x,y)$ shows a transformed image, L is total distinct grey levels, G and B are colour spaces of green and blue.

To improve the image quality, the researcher converted the original RGB image to Hue-Saturated-Value (HSV) colour space. After it, a threshold of HSV was multiplied by a Boolean mask of images computed by considering pixels values (Di Ruberto et al., 2020).

A researcher (Al-Tahhan et al., 2019) had processed his methodology in two steps. In their first step, they separated red, blue, and green colours from images. In the second step, they converted images into grayscale. Gray-scaled images are furthered passed for histogram equalisation and linear contrast stretching separately.

A researcher (Shree & Janani, 2019) had applied several pre-processing techniques on images to identify the WBC. Firstly, they converted the **RGB colour scheme** into a **CMYK**

colour. They applied contrast stretching, and after that, they applied the Gaussian filter to eliminate background noise.

The research has also converted RGB images into a CMYK colour system. After that, images with updated colour spaces are supplied to histogram equalisation, and thresholding (Abdeldaim et al., 2018)

Some researchers have changed the colour space from RGB to Greyscale, and further, they implemented median filtration to remove noise (Rawat, Singh, Bhaduria, et al., 2017; Rawat, Singh, Hs, et al., 2017).

Researchers have changed the colour space of resized RGB images to CMYK and applied L*a*b colour system (Vogado et al., 2016).

The author (Vincent et al., 2015), after acquiring the sample images, colour space is transformed from RGB to CIE L*a*b, which helps reduce the colour dimensions.

2.2: Segmentation

Segmentation helps a lot in detecting the WDCs from the image. Segmentation splits the images into meaningful information. In past literatures, researchers have used different segmentation techniques.

Segmentation plays a vital role to account accuracy. An author (Bodzas et al., 2020) used two steps methodology for image segmentation, which includes leukocyte localisation, and another is the extraction of the ‘f’ region. They both had four and three sub steps, respectively. In localisation, sub-step was thresholding three-phase filtration, adjacent cell detection, and finally, extraction of cells. At the same time, nucleus region extraction was done by nucleus localisation, nucleus extraction, and finally, cytoplasm extraction.

(Di Ruberto et al., 2020) extracted relevant information of leukocytes in steps of blob detection. After applying the Gaussian filter in the pre-processing step, scientists used the watershed algorithm to segmentation leukocytes. Researchers (Sukhia et al., 2019) used the diffused-expectations-maximisation (DEM) method that acquires two thresholds for the segmentation. Component of Gaussian mixture defines region class, and their parameters are approximated by using maximum feasibility approach.

Researcher (Al-Tahhan et al., 2019) proposed segmentation methodology in three steps; the first step was WBC extraction, and second step was nucleus extraction. In the first step, the researcher used a colour segmentation procedure to extract white blood cells. After that, in the second step, they used histogram equalisation and linear contrast stretching for the extraction of a nucleus.

Another researcher (Shree & Janani, 2019) used a colour-based clustering method for segmentation.

(Dharani & Hariprasath, 2018) used histogram equalisation on grayscale image for segmentation. To improve more accuracy, they further applied Otsu's algorithm.

The method of segmentation adopted by (Abdeldaim et al., 2018) was Zak's algorithm. Before proceeding towards Zak's algorithm, intensity values generated by histogram on the image dataset. After that, values of thresholding were produced by Zak's algorithm.

Scientist (Rehman et al., 2018) used a simple threshold method for segmentation. It is vital to get good results of segmentation to help better get good accuracy of the results of disease. To give better accuracy, scientist performs HSV in pre-processing. After that, they applied the maximum thresholding method.

Support Vector Machine (SVM) was used by the authors (Zhao et al., 2017), which significantly improved accuracy.

One of the crucial phases in the detection of images is segmentation for highly accurate classification. A researcher (Mishra et al., 2017) segmented microscopic images by colour based clustering.

Image segmentation was focused on this research. The authors used three different techniques for the process of segmentation, namely hue saturation value (HSV) based segmentation, watershed, and K-mean clustering algorithm (Jagadev & Virani, 2017).

Global thresholding is applied to the blood samples to extract different objects at the different intensities on pixels (Rawat, Singh, Bhaduria, et al., 2017)

In segmentation, writers (Vogado et al., 2016) used two colour space systems for the segmentation: CMYK and L*a*b of white blood.

K-mean clustering is used to extract the authors' leukocyte nuclei (Basima & Panicker, 2016; Goutam & Sailaja, 2015).

The writer had used ANN for the segmentation process. In their methodology, firstly, they have isolated the lymphocytic cells. Thereafter, they have isolated the nucleus of the leukaemia samples (Bhattacharjee & Saini, 2015)

Segmentation Sequential Neural Network was applied by an author (Vincent et al., 2015) to increase the system's performance.

The methodology (Vaghela et al., 2015) was two ways to segmentation white blood cells. WBC and the nucleus were done separately. WBC segmentation was accomplished by linear contrast stretching, and the nucleus was segmented through colour-based segmentation. In the colour-based segmentation method, they had used the Hue Saturation Intensity coloured model. For complete segmentation and improvement in accuracy, K-mean clustering was applied further on the image dataset.

2.3: Classification

Classification is a **critical phase** that compares the input test image results with the standardised values and decides which class's input data belongs. So, this phase separates the cancerous and non-cancerous images in our case study.

(Anwar & Alam, 2020) trained convolution neural network CNN architecture, which consists of ten layers. This architecture performed two significant tasks. The first task was feature extraction, and the second task was to classify the extracted features of an input image with learned CNN features.

To classify microscopic input images, researchers (Bodzas et al., 2020) imposed an artificial neural network (ANN) and the support vector machine (SVM).

Scientists (Di Ruberto et al., 2020) used the CCN model for feature extraction. After that, they used three linear support vector machine model for the classification of their dataset. The researchers (Kassani et al., 2019) proposed a hybrid architecture based on the CNN model. In this model, they used two pre-trained CNN models (MobileNet and VGG16). After performing both CNN models individually on the dataset, features from both models were concatenated into a single featured vector.

(Shree & Janani, 2019) used Support Vector Machines binary (SVM) to classify the images into their suitable classes. In this classifier, input data is transformed into a higher dimensional feature space; after that, the maximum margin hyperplane created by SVM is classified into suitable classes.

The researchers (Alsalem et al., 2019) proposed a decision matrix for the dataset classification. The decision matrix model consists of two main parts, which are decision and alternatives criteria.

(Abdeldaim et al., 2018) used multiple techniques for the classification of microscopic images. They used K-NN, SVM-RBF, SVM-L, SVM-P, NB-G, NBK and TREE on different scenarios, but K-NN achieved the best classification accuracy.

For classification, authors (Zhao et al., 2017) used multiple classifiers to classify images of WBCs. They manage to use SVM to extract high-level features; they used convolution neural networks, and lastly, they used a random forest algorithm.

For classification, (Rawat, Singh, Bhaduria, et al., 2017) tested multiple classifiers on microscopic images. They used support vector machines (SVM), smooth support vector machines (SSV), k-nearest neighbour, probabilistic neural network (PNN) and adaptive neuro-fuzzy inference (ANFI) system.

Researchers (Basima & Panicker, 2016; Goutam & Sailaja, 2015; Jagadev & Virani, 2017) used SVM for the classification of images. The classifier will classify microscopic images of leukaemia into either affected class or non-affected class.

(Rawat et al., 2015) used Support Vector Machines binary (SVM) to classify the images into their suitable classes. In this classifier, input data is transformed into a higher dimensional feature space; after that, the maximum margin hyperplane created by SVM is classified into suitable classes.

The authors (Vincent et al., 2015) proposed a Sequential Neural Network Architecture (SNN) because this technique is very famous based on accuracy and time efficiency. Their proposed methodology was based on two stages; however, authors could not perform both stages due to a lack of input images. Although they used one stage, their accuracy was 97.7%.

Table-2.1: Literature Review

Year	Author	Method	Results (%)
2015	(Bhattacharjee & Saini)	Segmentation: Morphological operators	96.67
		Classification: KNN, SVM, ANN, K-means	KNN: 95.23 SVM: 90.47 ANN: 95.23
			KM 85.71
2015	(Goutam & Sailaja)	Image Pre-Processing Stage: RGB to Grey Scale, Median filtering to reduce unwanted effects	F-Measure 93.44
		Segmentation	
		K-Mean Clustering	
		Classification	
		SVM	
2015	(Patel & Mishra)	Segmentation Zack Algorithm	93.57
		Classification	

SVM

2015	(Vincent, Kwon, Lee, & Moon)	Segmentation K-Means Clustering Classification SNN	SNN classification 97.7 Outperformed our referred publication with 93.5
2015	(Rawat et al., 2015)	Classification SVM	89.8
2016	(Basima & Panicker)	Segmentation K-Means Clustering Classification SVM	- 94.56
2016	(Jagadev & Virani, 2017)	Classification SVM	94.56
2017	(Mishra, Sharma, Majhi, & Sa)	Segmentation bounding box technique Classification NB, KNN, BPNN, and SVM	NB 81.66 (avg) KNN 83.46 (avg) BPNN 58.7 (avg) SVM 89.76 (avg)
2017	(Rawat, Singh, Bhadauria, et al., 2017)	Classification SVM, SSV, K-NN, PNN and ANFI	97.6
2017		Segmentation Global Thresholding	

	(Rawat, Singh, Bhaduria, et al., 2017)	Classification	80.0
		PCA-k-NN	92.3
		PCA-PNN	
		PCA-SSVM	83.8
		PCA- SVM	94.6
2017	(Zhao et al.)	Classification	Monocyte: 85.3
		SVM	Neutrophil 97.1
		Feature Extraction	Lymphocyte 74.7
		CNN	
		Recognition of other WBCs	
		RFM	
2018	(Abdeldaim et al.)	Classification: using a few texture features, three normalisation techniques (3NT)	KNN 95.78% (Grey-Scaling)
		Classification: using all texture features with 3NT	KNN 95.99% (Z- Score)
		Classification: colour features with 3NT	KNN 88.95% (Grey-Scaling)
		Classification: all colour features with 3NT	SVM-P 92.52% (Min-Max)
		Classification: colours and texture features with 3NT	KNN 96.42% (Grey-Scaling)

		Classification: colours, shape, and texture features with 3NT	KNN 96.01% (Grey-Scaling)
2018	(Rehman et al.)	Segmentation: STM	97.78 overall
		Classification: Alex- net	
2019	(Sukhia et al., 2019)	Classification Sparse Method (CNN based)	94
2019	(Shree & Janani, 2019)	Classification Alex-net model with CNN	90.30
2019	(Kassani et al., 2019)	Classification: CNN	95.17
2019	(Hegde et al., 2019)	Segmentation Arithmetic and morphological operations.	96.5 overall
		Classification Active Contours	
2020	(Di Ruberto et al., 2020)	Segmentation watershed	94.1 Classification of leukaemia
		Classification CNN & SVM	
2020	(Bodzas et al., 2020)	Classification ANN & SVM	Specificity: 95.31%

2020 (Anwar & Classification: 99.5
Alam, 2020) CNN

CHAPTER 03

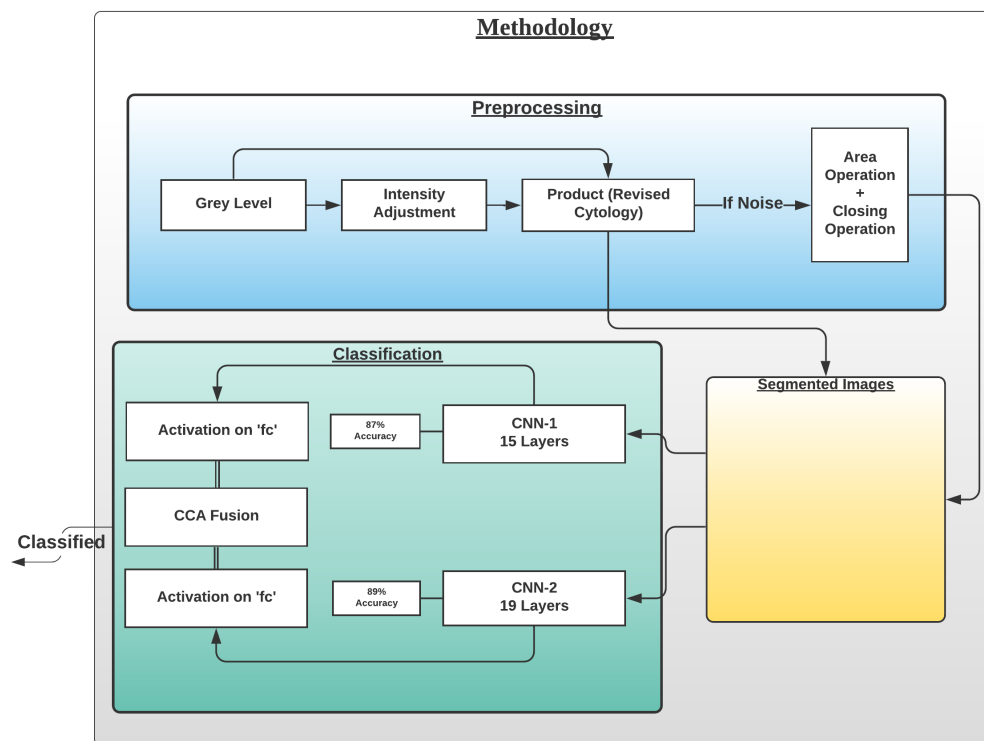
PROPOSED METHODOLOGY

3: Proposed Methodology

Nowadays, biomedical images play a significant part in identifying the disease, their treatments and research in health. Due to modern applications and technology, enhancement in biomedical images is censorious for analysing, diagnosing, and making clinical decisions.

In this research study, we proposed a deep learning-based, computer-aided system for blood cancer recognition using microscopic images, consisting of the following primary steps, as shown in Figure-3-1, where pre-processing is performed to improve the visibility of the lesion area. After pre-processing, image segmentation is performed to extract the region of interest. Later, hybrid CNN models are used for the classification of the lesion.

Figure-3.1: Proposed Architecture



3.1: Image Acquisitions

Microscopic images of blood gathered from Leukaemia Diagnostics at Munich University Hospital smear are acquired by 118 patients identified by different subtypes of AML. each image file contains a resolution of 400 by 400 px, a disk size is 640KB, and file format is “TIFF” (Clark et al., 2013; Matek et al., 2019). Moreover, we also gathered images from a public database of all challenge dataset of ISBI 2019 (Mohajerani & Ntziachristos, 2019; Shah et al., 2019). SN-AM Dataset: White Blood cancer dataset of B-ALL and MM for stain normalisation. In this dataset, we have collected images of B-ALL and MM of around 55 and 5 subjects respectively. The image’s size is 2560 by1920 pixels, and they all are in BMP format (Gupta et al., 2018, 2020; Natasha Honomichl, 2019b). Finally, we gathered a dataset from MiMM_SBILab Dataset: Microscopic Images of Multiple Myeloma of 5 subjects, these images are of 2560 by1920 pixels (Gupta et al., 2018, 2020; Natasha Honomichl, 2019a).

3.2: Image Pre-processing

Pre-processing is a procedure that is adopted to enhance the quality of images and increases visualisation. In medical imaging, image processing is a very crucial phase, which helps in improving the images. This can be one of the most critical factors to achieve good results and accuracy in the proceeding phases of image processing methodology. Medical images may contain a different issue that may lead to poor and low visualisation of the image. If the images are poor or of low quality, it may lead to unsatisfactory results.

Our methodology's first challenge was image pre-processing; we faced multiple challenges to meet the pre-processing phase, which involves multiple steps to enhance our dataset's quality of images. The main challenges were background removal, ripping out un-essential blood components, image enhancement and noise removal. The working of pre-processing on our sample images are shown in Figure-3-2. Our dataset consists of an RGB colour model. To encounter the image enhancement challenges. Firstly, we load our images in 'MATLAB' in the form of the matrix '*T*', as shown in Figure-3-2 (a). after that, we converted the colour space of our dataset and stored it in the matrix '*pout*', converted into the greyscale 8-bit mode, as shown in Figure-3-2 (b). After converting it into binary, we have enhanced the images using the image adjustment method and adaptive histogram equalisation (AHE) method. By applying image intensity adjustment and AHE, the contrast of the output images is increased as matrix '*pout_adapthisteq*'. It can be observed that the boundaries of the lesion have become more contrasted and prominent while, on the other hand, background, noise, and un-essential components have become fade, as shown below in Figure-3-2(c). After noticing the last pre-processing output, we observed that the images are a little bit blurred, and noise still exists in our dataset. To increase the structure and sharpness of images, we multiplied binary image '*pout*' with the output of enhanced image

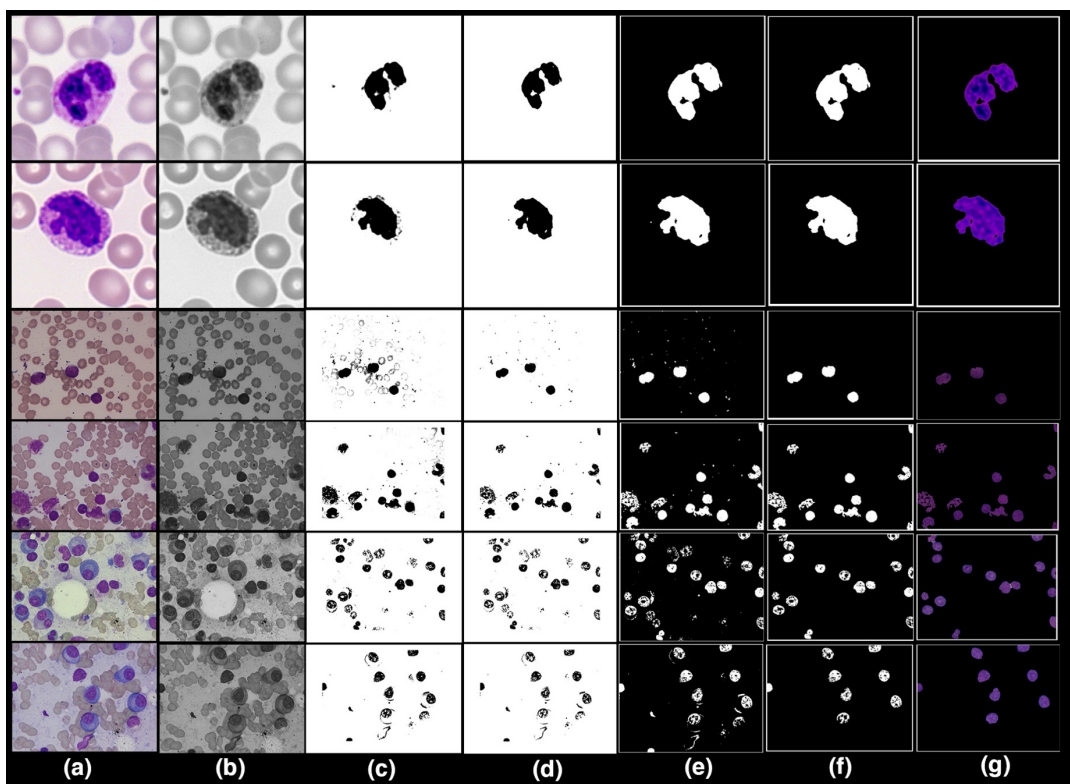
'pout_adapthisteq'; samples of this step are shown in Figure-3-2(d), and the result matrix is stored in variable 'poutnew'.

$$poutnew = pout \times pout_adapthisteq$$

In the next step, we have taken a complement of *poutnew* (image's matrix) to get the background in black colour and nucleus of blood in white colour as shown in Figure-3-2(e). In some image's dataset noticed background noise. We used area operation and closing operation to remove background noise, which has improved the lesion's boundaries, as shown in Figure-3-2(f). Finally, we multiply the final output gained by applying area and closing operation with the source image to regenerate the images dataset in RGB colour space, and we resize dataset images to [400,400] as shown in Figure-3-2(g).

After applying all methods and techniques, we have managed to get noiseless, non-blurred, sharped and segmented images of the lesion.

Figure-3.2: Samples of pre-processing



3.3: Data Augmentation

In several tasks, CNNs proved state-of-the-art performance. However, the amount of the training data has a significant impact on CNN performance. Collecting adequate clinical images is difficult due to data privacy concerns in the medical field. We used different data augmentation approaches to enhance the CNN performance, as recommended in previous research (Kassani & Kassani, 2019; Pham et al., 2018), such as contrast and brightness correction, horizontal and vertical flips, intensity modifications and rotation, to solve the issue of less dataset availability and minimize over-fitting challenges. The dataset's class distributions before and after data augmentation are shown in table given below.

Table 3.1: Data Augmentation

Types	Before	After
Acute lymphoblastic leukemia	31	293
Multiple Myeloma	114	301

3.4: Image Classification

Classification is a critical phase that compares the input test image results with the standardised values and decides which class's input data belongs. So, this phase separates the cancerous and non-cancerous images in our case study.

Nowadays, deep learning techniques are being used to build a faster and most reliable computer-aided system to work in artificial intelligence. Under the classification's phase, we have developed the Hybrid Deep Learning architecture to classify lesion. According to researchers in recent works, they presented different schemes to use the CNN models; the first way is to train the model using a large number of a dataset, and the other one is to use a pre-trained model which is done by transfer for learning (Tajbakhsh et al., 2016). Our proposed methodology has implemented a hybrid CNN model that trains the large dataset of images and then transfers the learning to the preceding blocks, which will be discussed later in this chapter.

3.5: Feature Fusion

In our research, the first step in classification is to determine the architecture of the hybrid Convolutional Neural Network (ConvNet/ CNN) and the model's training that realise on the dataset. Our research work has proposed two individual blocks of Convolutional Neural Networks named CNN-1 and CNN-2.

3.5.1: Convolution Neural Network Model CNN-1

Our first self-trained convolution neural network (CNN-1) consists of total 19 layers, which includes one input layer, 2-Dimensional convolutional layers are 4, 4 batch normalisation layers, ReLU layers are also 4, 2-Dimensional max-pooling

layers are 3 in total, and there is only one layer of fully connected, soft-max and classification layer. Detail The detail layers are given below in table 3.1. The model of CNN-1 architecture is given in Figure-3.3.

Table-3.2: Layered Architecture of CNN-1

Layers
Input Layer
Convolution Layer 1
Batch-Normalization Layer 1
ReLU Layer 1
Max-Pooling Layer1
Convolution Layer 2
Batch-Normalization Layer 2
ReLU Layer 2
Max-Pooling Layer 2
Convolution Layer 3
Batch-Normalization Layer 3
ReLUlayer 3
Convolution Layer 4
Batch-Normalization Layer 4
ReLUlayer 4
Fully-Connected Layer
Softmax Layer
Classification Layer

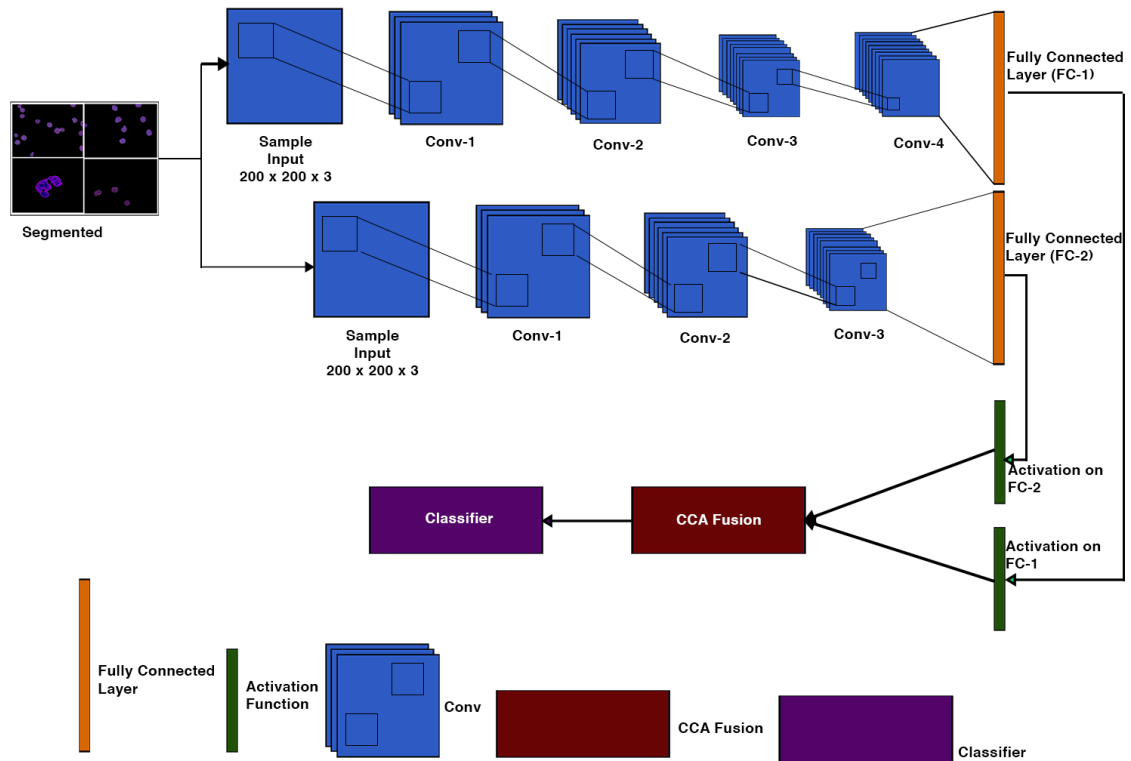
3.5.2: Convolution Neural Network CNN-2

In our second trained Convolution Neural Network (CNN-2), that consists of total 15 layers, which includes one input layer, 2-Dimensional convolutional layers are 3, 3 batch normalisation layers, ReLU layers are also 3, 2-Dimensional max-pooling layers are 2, and there is only one layer of fully connected, soft-max and classification layer as shown in the table given below. Also, the model of CNN-1 architecture is given below in Figure-3.3.

Table-3.3: Layered Architecture of CNN-2

Layers
Input Layer
Convolution Layer 1
Batch-Normalization Layer 1
ReLU Layer 1
Max-Pooling Layer1
Convolution Layer 2
Batch-Normalization Layer 2
ReLU Layer 2
Max-Pooling Layer 2
Convolution Layer 3
Batch-Normalization Layer 3
ReLU Layer 3
Fully-Connected Layer
Softmax Layer
Classification Layer

Figure-3.3: CNN-1 and CNN-2 Architecture



3.5.3: Feature Extraction using CNN-1 & CNN-2

The essential part of the model is feature extraction. In our methodology, we have trained a specific hybrid model for feature extraction. Our models (CNN-1 & CNN-2) are based on the sequence of conv, which has encapsulated 2-Dimensional convolutional layers, batch normalisation layers, ReLU layers, and 2-Dimensional max-pooling layers. Dataset is passed to each layer of conv by applying filters. Each conv extracts relevant information until the last max-pooling. Lastly, feature extraction is done on both networks by using a fully connected layer.

3.5.4: Self-Convolution Neural Network Transfer Learning

Convolution neural networks may take several days or even weeks to train a large amount of dataset. To reduce the time complexity of the afore-cited problem, we have addressed transfer learning. Transfer Learning is the process in which a trained model on a particular problem is used in such a way that it helps in the problem-solving of other co-related problem (Brownlee, 2019). We have used the *SoftMax* layer for activation function to achieve the objective of transfer learning for each CNN model of our architecture, as shown in Figure-3.3.

3.6: CCA Fusion

The method of merging two feature vectors to create a new feature vector that is more discriminative than either of the input feature vectors is known as feature fusion (Haghigat et al., 2016).

There are various methodologies for integrating CCA functions. One approach is to merge two sets of feature vectors into a single union-vector, after which features are extracted in a higher-dimensional real vector space. Another method is to use a complex vector to merge two feature vectors and then extract features from the complex vector space. Both feature fusion approaches seek to increase recognition rate; the union vector approach is known as serial feature fusion. The method based on the complex vector is known as parallel feature fusion (Sun et al., 2004). We have implemented the second approach to fuse the complex featured vectors CCN-1 and CNN-2. After the concatenation of both complex vectors, the output (*most discriminative vector features*) is passed to the classifier.

3.7: Classification

The final stage of a model's development is classification, aiming to predict the lesion category (Ali et al., 2019; Bagasjvara et al., 2016). The multi-class classification technique has been used in our proposed approach to characterise the input image based on the selected features. We used machine learning algorithms to compute the classification; the reason to do this was to reduce computation time. Bagging Ensemble, Linear Programming Boost (LPBoost), Total Boost Ensemble, K-Nearest Neighbour (K-NN), Fine K-Nearest Neighbour (FK-NN), RUSBoost, Coarse K-Nearest Neighbour (Coarse K-NN), and Support Vector Machine (SVM) are some of the classifiers; we have used in our proposed methodology. In our research, the best-reported classification results are computed by Bagging Ensemble, Linear Programming Boost (LPBoost).

CHAPTER 04

EXPERIMENTAL SETUP AND RESULTS

4: Experimental setup and Results

The experimental findings of the proposed hybrid model classification methodology are presented in both qualitative and quantitative aspects. We placed the proposed method to the test using the data we gathered.

4.1: Dataset

We collected a dataset from a public directory of around 4150 images. Our dataset consists of 3 classes, namely acute lymphoblastic leukaemia (ALL), acute myeloid leukaemia (AML), and multiple myeloma (MM). Initially, dataset contains 31 images of ALL, 4013 images of AML and 114 images of MM. After performing data augmentation on ALL and MM to resolve the issue of data overfitting, we got 293 images of ALL and 301 images of MM for classification. Furthermore, total number of images in AML class were too much as compared to other classes, which makes class unbalancing problem and may lead to biasness in the results. To coup-up with class unbalancing issue, we chose 307 random images of AML class. For classification, we divided datasets into 70 ratios 30, training and testing sets, which means we used 70% of the random images for training purpose and 30% of random images for testing purpose as shown in table 4.1.

Table 4.1: No. of samples used for classification

Types	Training	Testing	No of Samples
Acute lymphoblastic leukemia	205	88	293
Acute myeloid leukaemia	215	92	307
Multiple Myeloma	211	90	301

The proposed classification algorithms are compared to state-of-the-art classification algorithms like ANN & SVM, CNN & SVM, Active Contours and Alexnet. Well-known performance parameters such as sensitivity, precision, accuracy, F1 score, false-negative rates (FNR), and false-positive rates (FPR) are used to evaluate these classifiers.

4.2: Experimental Setup

For this research, experiments were carried out on a Microsoft Azure Server running on a 64-bit version of Windows 10 in MATLAB 2020b. The computer had an Intel Xeon Processor, 16 GB of RAM, and 130 GB of storage.

4.3: Features Extraction Results using CNN-1

This section will discuss the findings of feature extraction using the Convolutional Neural Network (CNN-1). We found that the accuracy gained by CNN-1 for individual classes ALL, AML, and MM are 77.27%, 98.91% and 92.22%, respectively. The discrete statistics of CNN-1 upon ALL, AML and MM, are cited below in table 4.2.

Table-4.2: Statistics of CNN-1 Model of Individual Classes

Class	Accuracy %	Sensitivity %	Specificity %	Precision %	False Positive Rate %	F1 Score %
ALL	77.273	77.273	96.154	90.667	3.8462	83.436
AML	98.913	98.913	98.315	96.809	1.6854	97.849
MM	92.222	92.222	90	82.178	10	86.911

Overall accuracy gained by CNN-1 on ALL, AML and MM was 89.63%. The overall statistics of CNN-1 are given below in the table 4.3.

Table-4.3: CNN-1 Combined Statistics of All Classes

Statistics	Result in %
Accuracy	89.63
Sensitivity	89.47
Specificity	94.82
Precision	89.88
False Positive Rate	5.18

The confusion matrix of CNN-1 is shown below.

Figure-4.1: Confusion Matrix of CNN-1 Feature Extraction

Confusion matrix CNN-1					
True Class	ALL	ALL	77.3%	22.7%	
	AML	AML	98.9%	1.1%	
	MM	MM	92.2%	7.8%	
		90.7%	96.8%	82.2%	
		9.3%	3.2%	17.8%	
Predicted Class					
ALL		AML		MM	

4.4: Features Extraction Results using CNN-2

In this section, we will discuss the findings of feature extraction using the Convolutional Neural Network (CNN-2). We discovered that CNN-2 achieves 77.27 percent, 98.91 %, and 92.22 percent accuracy for individual classes ALL, AML, and MM, respectively. The statistics of CNN-2 upon ALL, AML, and MM, are mentioned below in table 4.4.

Table-4.4: Statistics of CNN-2 Model of Individual Classes

Class	Accuracy %	Sensitivity %	Specificity %	Precision %	False Positive Rate %	F1 Score %
ALL	70.455	70.455	95.604	88.571	4.3956	78.481
AML	98.913	98.913	100	100	0	99.454
MM	92.222	92.222	85.556	76.147	14.444	83.417

Overall accuracy gained by CNN-1 on ALL, AML and MM was 87.41%. The overall statistics of CNN-2 are given below in the table 4.5

Table-4.5: CNN-2 Combined Statistics of All Classes

Statistics	Result in %
Accuracy	87.41
Sensitivity	87.20
Specificity	93.72
Precision	88.24
False Positive Rate	6.28
F1 score	87.12

The confusion matrix of CNN-2 is shown below in Figure-4-2.

Figure-4.2: Confusion Matrix of CNN-2 Feature Extraction

Confusion matrix CNN-2			
True Class	ALL	26	
	70.5%	29.5%	
	98.9%	1.1%	
MM	7	83	
	88.6%	100.0%	76.1%
	11.4%		23.9%
	ALL	AML	MM
	Predicted Class		

4.5: Classification Results using CCA Fusion

In the past chapter, we discussed the proposed methodology that the features extracted by CNN-1 and CNN-2 are concatenated into a single enhanced vector through Canonical Correlation Analysis (CCA) Fusion. After that, the fused vectors of enhanced features were passed out to the classifiers to classify the input images. Bagging Ensemble, Total Boost Ensemble, Fine K-Nearest Neighbour (FK-NN), RUSBoost, Coarse K-Nearest Neighbour (Coarse K-NN), and Support Vector Machine (SVM) are some of the classifiers; used in the proposed methodology. We have implemented multiple classifiers of machine learning in this step. The reason behind this was to minimise the whole system's execution time as much as possible.

4.5.1: Statistical Analysis of Bagging Ensemble on CCA Fusion

We have used the Bagging Ensemble classifier to classify the lesion on the vector of the fused feature. The statistics show that the AML class's accuracy is 100 percent, ALL reached the accuracy of 93.182 percent, and MM's accuracy is gained around 97.78 percent. Sensitivity, precision, F1-score etc., are cited below in table 4.6. The overall accuracy of this classifier was very efficient and reached 97.4 percent. The overall combined results of the three classes are also shown in table 4.7, which is also given below; also, the confusion matrix is shown in Figure-4-3.

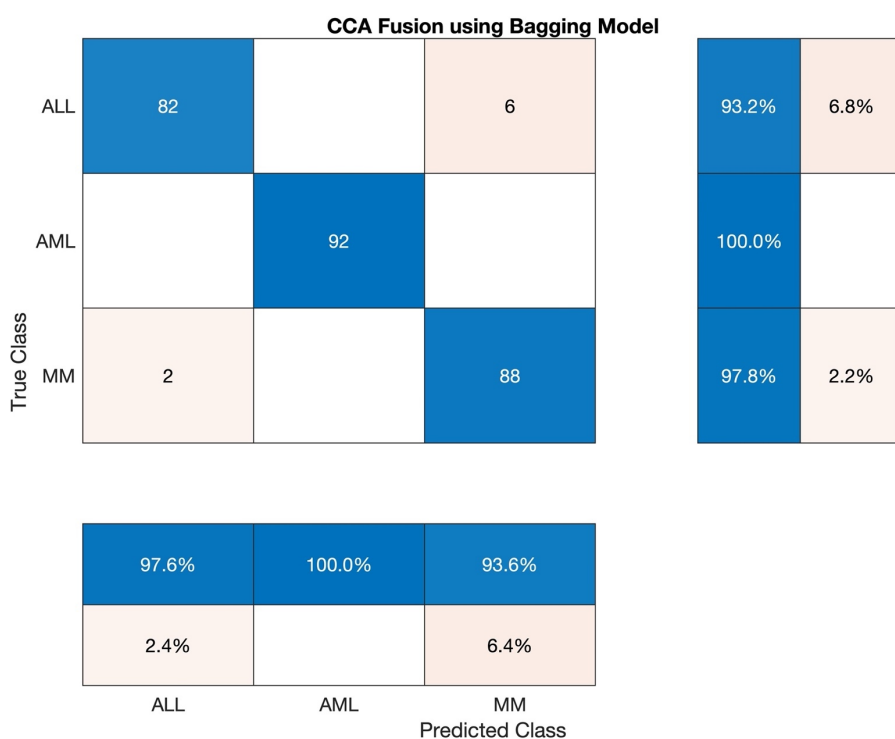
Table-4.6: Statistics of Bagging Model using CCA Fusion

Class	Accuracy %	Sensitivity %	Specificity %	Precision %	False Positive Rate %	F1 Score %
ALL	93.182	93.182	98.901	97.619	1.0989	95.349
AML	100	100	100	100	0	100
MM	97.778	97.778	96.667	93.617	3.333	95.652

Overall accuracy gained by Bagging Ensembler on ALL, AML and MM was 97.04%. The overall statistics of Bagging Ensembler are given below in the table 4.7

Table-4.7: Overall Statistics of Bagging Model using CCA Fusion

Statistics	Result in %
Accuracy	97.04
Sensitivity	96.99
Specificity	98.52
Precision	97.0
False Positive Rate	1.48
F1 score	97.00

Figure-4.3: Confusion Matrix of Bagging Model

4.5.2: Statistical Analysis of Total Boost Model on CCA Fusion

We have used Total Boost classifier to classify the lesion on vector of fused feature. The statistics shows that the accuracy of AML class is 100 percent, ALL reached the accuracy of 92.045 percent, and accuracy of MM is gained around 97.78 percent. Sensitivity, precision, F1-score etc are cited below in the table 4.8. Overall accuracy of this classifier was very efficient and reached to 96.67 percent. The overall combined results of three classes are also shown in table 4.9 which is also given below, also confusion matrix are shown in Figure-4-4.

Table-4.8: Statistics of Total Boost Model using CCA Fusion

Class	Accuracy %	Sensitivity %	Specificity %	Precision %	False Positive Rate %	F1 Score %
ALL	92.045	92.045	98.901	97.59	1.0989	94.737
AML	100	100	100	100	0	100
MM	97.778	97.778	96.111	92.632	3.8889	95.135

Overall accuracy gained by Total Boost Model on ALL, AML and MM was 96.67%. The overall statistics of Total Boost Model are given below in the table 4.9

Table-4.9: Overall Statistics of Total Boost Model using CCA Fusion

Statistics	Result in %
Accuracy	96.67
Sensitivity	96.62
Specificity	98.34
Precision	96.74
False Positive Rate	1.66
F1 score	96.62

Figure-4.4: Confusion Matrix of Total Boost Model

CCA Fusion using Total Boost Model					
True Class	ALL	AML	MM		
	81	92	88	92.0%	8.0%
ALL				100.0%	
AML				97.8%	2.2%
MM	2				
Predicted Class		ALL	AML	MM	
97.6%		100.0%		92.6%	
2.4%				7.4%	

4.5.3: Statistical Analysis of Fine-KNN on CCA Fusion

In this section we tested Fine KNN classifier to classify the lesion on vector of fused feature. The statistics shows that the accuracy of AML class is 100 percent, ALL reached the accuracy of 92.045 percent, and accuracy of MM is gained around 95.56 percent. Sensitivity, precision, F1-score etc are cited below in the table 4.10. Overall accuracy of this classifier was very efficient and reached to 95.93 percent. The overall combined results of three classes are also shown in table 4.11 which is also given below, also confusion matrix are shown in Figure-4-5.

Table-4.10: Statistics Fine KNN using CCA Fusion

Class	Accuracy %	Sensitivity %	Specificity %	Precision %	False Positive Rate %	F1 Score %
ALL	92.045	92.045	97.802	95.294	2.1978	93.642
AML	100	100	100	100	0	100
MM	95.556	95.556	96.111	92.473	3.8889	93.989

Overall accuracy gained by Fine KNN on ALL, AML and MM was 95.93%. The overall statistics of Fine KNN are given below in the table 4.10

Table-4.11: Overall Statistics Fine KNN using CCA Fusion

Statistics	Results in %
Accuracy	95.93
Error	4.07
Sensitivity	95.87
Specificity	97.97
Precision	95.92
False Positive Rate	2.03
F1_score	95.88
Matthews Correlation Coefficient	93.87

Figure-4.5: Confusion Matrix of F-KNN

CCA Fusion using F-KNN				
True Class	ALL	81		7
	AML		92	
	MM	4		86
		95.3%	100.0%	92.5%
		4.7%		7.5%
Predicted Class				
ALL				
AML				
MM				

4.5.4: Statistical Analysis of Medium-KNN on CCA Fusion

We also have tested Medium KNN classifier to classify the lesion on the vector of the fused feature. The statistics show that the AML class's accuracy is 100 percent, ALL reached the accuracy of 92.045 percent, and MM's accuracy is gained around 96.67 percent. Sensitivity, precision, F1-score etc., are cited below in table 4.12. The overall accuracy of this classifier was very efficient and reached 96.30 percent. The three classes' overall combined results are also shown in table 4.13, which is also given below; also, the confusion matrix is shown in Figure-4-6.

Table-4.12: Statistics of Medium KNN using CCA Fusion

Class	Accuracy %	Sensitivity %	Specificity %	Precision %	False Positive Rate %	F1 Score %
ALL	92.045	92.045	98.352	96.429	1.6484	094.186
AML	100	100	100	100	0	100
MM	96.667	96.667	96.111	92.553	3.8889	94.565

Overall accuracy gained by Medium KNN on ALL, AML and MM was 96.30%.

The overall statistics of Medium KNN are given below in the table 4.13

Table-4.13: Overall Statistics of Medium KNN using CCA Fusion

Statistics	Results in %
Accuracy	96.30
Error	3.70
Sensitivity	96.24
Specificity	98.15
Precision	96.33
False Positive Rate	1.85
F1_score	96.25
Matthews Correlation Coefficient	94.44

Figure-4.6: Confusion Matrix of Medium KNN

CCA Fusion using Medium-KNN			
True Class	ALL	AML	MM
	81	92	87
	92.0%	100.0%	96.7%
Predicted Class	ALL	AML	MM
96.4%	100.0%	92.6%	3.6%
			7.4%

4.5.5: Statistical Analysis of Coarse-KNN on CCA Fusion

We also have tested the Coarse KNN classifier to classify the lesion on the vector of the fused feature. The statistics show that the AML class's accuracy is 96.739 percent, ALL reached the accuracy of 90.909 percent, and MM's accuracy is gained around 97.778 percent. Sensitivity, precision, F1-score etc., are cited below in table 4.14. The overall accuracy of this classifier was very efficient and reached 95.19 percent. The three classes' overall combined results are also shown in table 4.15, which is also given below; also, the confusion matrix is shown in Figure-4-7.

Table-4.14: Statistics of Coarse KNN using CCA Fusion

Class	Accuracy %	Sensitivity %	Specificity %	Precision %	False Positive Rate %	F1 Score %
ALL	90.909	90.909	98.901	97.561	1.0989	92.486
AML	96.739	96.739	100	100	0	98.343
MM	97.778	97.778	93.889	88.889	6.1111	93.122

Overall accuracy gained by Coarse KNN on ALL, AML and MM was 95.19%. The overall statistics of Coarse KNN are given below in the table 4.15

Table-4.15: Overall Statistics of Coarse KNN using CCA Fusion

Statistics	Results in %
Accuracy	95.19
Error	4.81
Sensitivity	95.14
Specificity	97.60
Precision	95.48
False Positive Rate	2.40
F1_score	95.19
Matthews Correlation Coefficient	0.9292

Figure-4.7: Confusion Matrix of Coarse KNN

CCA Fusion using Coarse-KNN			
True Class	ALL	80	8
	AML	89	3
	MM	2	88
	90.9%	9.1%	
96.7%	3.3%		
97.8%	2.2%		
97.6%	100.0%	88.9%	
2.4%		11.1%	
Predicted Class			
ALL		MM	

4.5.6: Statistical Analysis of SVM on CCA Fusion

In this section, we have discussed the reported statistics of the most famous traditional machine learning algorithm. Support Vector Machine (SVM) classifier to classify the lesion on the vector of the fused feature. The statistics show that the accuracy of the AML class is 100 percent, ALL reached the accuracy of 90.909 percent, and MM's accuracy is gained around 94.44 percent. Sensitivity, precision, F1-score etc., are cited below in table 4.16. The overall accuracy of this classifier was very efficient and reached 95.19 percent. The overall combined results of the three classes are also shown in table 4.17, which is also given below; also, the confusion matrix is shown in Figure-4-8.

Table-4.16: Statistics of SVM using CCA Fusion

Class	Accuracy %	Sensitivity %	Specificity %	Precision %	False Positive Rate %	F1 Score %
ALL	90.909	90.909	97.253	94.118	2.7473	92.486
AML	100	100	100	100	0	100
MM	94.444	94.444	95.556	91.398	4.4444	92.896

Overall accuracy gained by SVM on ALL, AML and MM was 95.19%. The overall statistics of SVM are given below in the table 4.17.

Table-4.17: Overall Statistics of SVM using CCA Fusion

Statistics	Results in %
Accuracy	95.19
Error	4.81
Sensitivity	95.12
Specificity	97.60
Precision	95.17
False Positive Rate	2.40
F1_score	95.13
Matthews Correlation Coefficient	92.75

Figure-4.8: Confusion Matrix of SVM

		CCA Fusion using SVM		
		ALL	AML	MM
True Class	ALL	80		8
	AML		92	
	MM	5		85
		90.9%	9.1%	
		100.0%		
		94.4%	5.6%	
		94.1%	100.0%	91.4%
		5.9%		8.6%
		ALL	AML	MM
		Predicted Class		

4.5.7: Statistical Analysis of LPBoost model on CCA Fusion

This section has discussed the reported statistics of the most famous traditional machine learning algorithm, LPBoost model classifier, to classify the lesion on the vector of the fused feature. The statistics show that the accuracy of AML class is 100 percent, ALL reached the accuracy of 93.182 percent, and accuracy of MM is gained around 95.556 percent. Sensitivity, precision, F1-score etc are cited below in table 4.18. This classifier's overall accuracy was very efficient and reached 96.30 percent, which is also shown in Table-4.19 given below; also, the confusion matrix on CCA fusion is shown in Figure-4-9.

Table 4.18: Statistics of LPBoost using CCA Fusion

Class	Accuracy %	Sensitivity %	Specificity %	Precision %	False Positive Rate %	F1 Score %
ALL	93.182	93.182	97.802	95.349	2.1978	94.253
AML	100	100	99.438	98.925	0.5618	99.459
MM	95.556	95.556	97.222	94.505	2.7778	95.028

Overall accuracy gained by LPBoost on ALL, AML and MM was 96.30%. The overall statistics of LPBoost are given below in the table 4.19

Table 4.19: Overall Statistics of LPBoost using CCA Fusion

Statistics	Results in %
Accuracy	96.30
Error	3.70
Sensitivity	96.25
Specificity	98.15
Precision	96.26
False Positive Rate	1.85
F1_score	96.25
Matthews Correlation Coefficient	94.41

Figure 4.9: Confusion Matrix of LPBoost Model

CCA Fusion using LPBoost Model					
True Class	ALL	AML	MM		
	82	1	5	93.2%	6.8%
ALL		92		100.0%	
MM	4		86	95.6%	4.4%
				95.3%	98.9%
				4.7%	1.1%
				94.5%	5.5%
Predicted Class					

4.5.8: Statistical Analysis of RUSBoost on CCA Fusion

This section has discussed the reported statistics of the most famous traditional machine learning algorithm, RUSBoost classifier, to classify the lesion on the vector of the fused feature. The statistics show that the accuracy of AML class is 100 percent, ALL reached the accuracy of 90.909 percent, and accuracy of MM is gained around 94.45 percent. Sensitivity, precision, F1-score etc are cited below in table 4.21. This classifier's overall accuracy was very efficient and reached 96.30 percent, which is also shown in Table-4.22 given below; also, the confusion matrix on CCA fusion is shown in Figure-4-10.

Table-4.20: Statistics of RUSBoost using CCA Fusion

Class	Accuracy %	Sensitivity %	Specificity %	Precision %	False Positive Rate %	F1 Score %
ALL	90.909	90.909	98.901	97.561	1.0989	94.118
AML	100	100	100	100	0	100
MM	94.444	94.444	95.556	91.398	4.4444	92.896

Overall accuracy gained by RUSBoost on ALL, AML and MM was 96.30 %. The overall statistics of RUSBoost are given below in the table 4.22

Table-4.21: Overall Statistics of RUSBoost using CCA Fusion

Statistics	Results in %
Accuracy	96.30
Error	3.70
Sensitivity	96.23
Specificity	98.15
Precision	96.41
False Positive Rate	1.85
F1_score	96.25
Matthews Correlation Coefficient	94.49

Figure 4.10: Confusion Matrix of RUSboost

CCA Fusion using RUSboostmodel		
True Class	ALL	AML
	80	92
	2	88
Predicted Class		
ALL	97.6%	100.0%
AML	2.4%	8.3%
MM	91.7%	90.9%

4.6: Classification Results using Serial Fusion

After fusing using CCA, we also have traced other technique of featured concatenation. The features extracted by CNN-1 and CNN-2 are also concatenated into a single enhanced vector through Serial Fusion. After that, the fused vectors of enhanced features were passed out to the classifiers to classify the input images. Bagging Ensemble, Total Boost Ensemble, Fine K-Nearest Neighbour (FK-NN), RUSBoost, LPBoost Coarse K-Nearest Neighbour (Coarse K-NN), and Support Vector Machine (SVM) are some of the classifiers; used in the proposed methodology. We have implemented multiple classifiers of machine learning in this step.

4.6.1: Statistical Analysis of SVM on Serial Fusion

This section has discussed the reported statistics of the most famous traditional machine learning algorithm, SVM classifier, to classify the lesion on the vector of the fused feature. The statistics show that the accuracy of AML class is 100 percent, ALL reached the accuracy of 90.909 percent, and accuracy of MM is gained around 96.667 percent. Sensitivity, precision, F1-score etc are cited below in table 4.22. The confusion matrix on Serial fusion is shown in Figure-4-11.

Table 4.22: Statistics of SVM using Serial Fusion

Class	Accuracy %	Sensitivity %	Specificity %	Precision %	False Positive Rate %	F1 Score %
ALL	90.909	90.909	98.352	96.386	1.6484	93.567
AML	100	100	100	100	0	100
MM	96.667	96.667	95.556	91.579	4.4444	94.054

Overall accuracy gained by SVM on ALL, AML and MM was 95.93 %. The overall statistics of SVM are given below in the table 4.23

Table 4.23: Overall Statistics of SVM using Serial Fusion

Statistics	Results in %
Accuracy	95.93
Error	4.07
Sensitivity	95.86
Specificity	97.97
Precision	95.99
False Positive Rate	2.03
F1_score	95.87
Matthews Correlation Coefficient	93.90

Figure 4.11: Confusion Matrix of SVM



4.6.2: Statistical Analysis on Fine KNN Serial Fusion

This section has discussed the reported statistics of the most famous traditional machine learning algorithm, Fine KNN classifier, to classify the lesion on the vector of the fused feature. The statistics show that the accuracy of AML class is 99.43 percent, ALL reached the accuracy of 94.318 percent, and accuracy of MM is gained around 94.44 percent. Sensitivity, precision, F1-score etc are cited below in table 4.24. The confusion matrix on Serial fusion is shown in Figure-4-12.

Table 4.24: Statistics of Fine KNN using Serial Fusion

Class	Accuracy %	Sensitivity %	Specificity %	Precision %	False Positive Rate %	F1 Score %
ALL	94.318	94.318	97.802	95.402	2.1978	94.857
AML	99.43	99.43	99.43	98.925	0.5618	99.459
MM	94.444	95.556	97.222	94.444	2.7778	94.444

Overall accuracy gained by Fine KNN on ALL, AML and MM was 96.30 %. The overall statistics of Fine KNN are given below in the table 4.25

Table 4.25: Overall Statistics of Fine KNN using Serial Fusion

Statistics	Results in %
Accuracy	96.30
Error	3.70
Sensitivity	96.25
Specificity	98.15
Precision	96.26
False Positive Rate	1.85
F1_score	96.25
Matthews Correlation Coefficient	94.41

Figure 4.12: Confusion Matrix of Fine KNN

Serial Fusion using Fine KNN		
True Class	ALL	ALL
	AML	92
	MM	85
	94.3%	5.7%
	100.0%	
	94.4%	5.6%
Predicted Class		
	95.4%	98.9%
	4.6%	1.1%
	94.4%	5.6%

4.6.3: Statistical Analysis of Medium KNN on Serial Fusion

This section has discussed the reported statistics of the most famous traditional machine learning algorithm, Medium KNN classifier, to classify the lesion on the vector of the fused feature. The statistics show that the accuracy of AML class is 100 percent, ALL reached the accuracy of 89.773 percent, and accuracy of MM is gained around 97.78 percent. Sensitivity, precision, F1-score etc are cited below in table 4.26. The confusion matrix on Serial fusion is shown in Figure-4-13.

Table 4.26: Statistics of Medium KNN using Serial Fusion

Class	Accuracy %	Sensitivity %	Specificity %	Precision %	False Positive Rate %	F1 Score %
ALL	89.773	89.773	98.901	97.531	1.0989	93.491
AML	100	100	100	100	0	100
MM	97.778	97.778	95	90.722	0.05	94.118

Overall accuracy gained by Medium KNN on ALL, AML and MM was 95.93 %.

The overall statistics of Medium KNN are given below in the table 4.27

Table 4.27: Overall Statistics of Medium using Serial Fusion

Statistics	Results in %
Accuracy	95.93
Error	4.07
Sensitivity	95.86
Specificity	97.97
Precision	95.99
False Positive Rate	2.03
F1_score	95.87
Matthews Correlation Coefficient	93.90

Figure 4.13: Confusion Matrix of Medium KNN

Serial Fusion using Medium KNN			
True Class	ALL	9	
	89.8%	10.2%	
	100.0%		
MM	2	88	
	97.5%	100.0%	90.7%
	2.5%		9.3%
	ALL	AML	MM
	Predicted Class		

4.6.4: Statistical Analysis of RUSBoost on Serial Fusion

This section has discussed the reported statistics of the most famous traditional machine learning algorithm, RUSBoost classifier, to classify the lesion on the vector of the fused feature. The statistics show that the accuracy of AML class is 98.913 percent, ALL reached the accuracy of 88.636 percent, and accuracy of MM is gained around 94.444 percent. Sensitivity, precision, F1-score etc are cited below in table 4.28. The confusion matrix on Serial fusion is shown in Figure-4-14.

Table 4.28: Statistics of RUSBoost using Serial Fusion

Class	Accuracy %	Sensitivity %	Specificity %	Precision %	False Positive Rate %	F1 Score %
ALL	88.636	88.636	97.253	93.976	02.7473	91.228
AML	98.913	98.913	98.876	97.849	01.1236	98.378
MM	94.444	94.444	95	90.426	05	92.391

Overall accuracy gained by RUSBoost on ALL, AML and MM was 94.07 %. The overall statistics of RUSBoost are given below in the table 4.29.

Table 4.29: Overall Statistics of RUSBoost using Serial Fusion

Statistics	Results in %
Accuracy	94.07
Error	05.93
Sensitivity	94.00
Specificity	97.04
Precision	94.08
False Positive Rate	02.96
F1_score	94.00
Matthews Correlation Coefficient	91.10

Figure 4.14: Confusion Matrix of RUSBoost

Serial Fusion using RUSBoost			
True Class	ALL	ALL	
	AML	AML	
	MM	MM	
	78	2	8
			88.6% 11.4%
	91	1	98.9% 1.1%
	5	85	94.4% 5.6%
	94.0% 6.0%	97.8% 2.2%	90.4% 9.6%
	ALL	AML	MM
	Predicted Class		

4.6.5: Statistical Analysis of TotalBoost on Serial Fusion

This section has discussed the reported statistics of the most famous traditional machine learning algorithm, TotalBoost classifier, to classify the lesion on the vector of the fused feature. The statistics show that the accuracy of AML class is 100 percent, ALL reached the accuracy of 93.182 percent, and accuracy of MM is gained around 93.3 percent. Sensitivity, precision, F1-score etc are cited below in table 4.30. The confusion matrix on Serial fusion is shown in Figure-4-15.

Table 4.30: Statistics of TotalBoost using Serial Fusion

Class	Accuracy %	Sensitivity %	Specificity %	Precision %	False Positive Rate %	F1 Score %
ALL	93.182	93.182	96.703	93.182	3.2967	93.182
AML	100	100	100	100	0	100
MM	93.333	93.333	96.667	93.333	3.3333	93.333

Overall accuracy gained by TotalBoost on ALL, AML and MM was 95.56 %. The overall statistics of TotalBoost are given below in the table 4.31

Table 4.31: Overall Statistics of TotalBoost using Serial Fusion

Statistics	Results in %
Accuracy	95.56
Error	4.44
Sensitivity	95.51
Specificity	97.79
Precision	95.51
False Positive Rate	02.21
F1_score	95.51
Matthews Correlation Coefficient	93.30

Figure 4.15: Confusion Matrix of Total Boost

Serial Fusion using Total Boost		
True Class	ALL	MM
	82	92
	6	84
ALL	93.2%	100.0%
AML	6.8%	6.7%
MM	93.3%	6.7%
Predicted Class		

4.6.6: Statistical Analysis of LPBoost on Serial Fusion

This section has discussed the reported statistics of the most famous traditional machine learning algorithm, LPBoost classifier, to classify the lesion on the vector of the fused feature. The statistics show that the accuracy of AML class is 100 percent, ALL reached the accuracy of 94.318 percent, and accuracy of MM is gained around 95.56 percent. Sensitivity, precision, F1-score etc are cited below in table 4.32. The confusion matrix on Serial fusion is shown in Figure-4-16.

Table 4.32: Statistics of LPBoost using Serial Fusion

Class	Accuracy %	Sensitivity %	Specificity %	Precision %	False Positive Rate %	F1 Score %
ALL	94.318	94.318	97.802	95.402	2.1978	94.857
AML	100	100	100	100	0	100
MM	95.556	95.556	97.222	94.505	2.7778	95.028

Overall accuracy gained by LPBoost on ALL, AML and MM was 96.67 %. The overall statistics of LPBoost are given below in the table 4.33

Table 4.33: Overall Statistics of LPBoost using Serial Fusion

Statistics	Results in %
Accuracy	9667
Error	333
Sensitivity	9662
Specificity	9834
Precision	9664
False Positive Rate	1.66
F1_score	96.63
Matthews Correlation Coefficient	94.97

Figure 4.16: Confusion Matrix of LPBoost

Serial Fusion using LPBoost			
True Class	ALL	ALL	
	AML	AML	
	MM	MM	
	82	6	93.2% 6.8%
	92		100.0%
	5	85	94.4% 5.6%
			94.3% 100.0% 93.4%
	ALL	AML	MM
			Predicted Class

4.6.7: Statistical Analysis of Bagging Ensembler on Serial Fusion

This section has discussed the reported statistics of the most famous traditional machine learning algorithm, Bagging Ensembler classifier, to classify the lesion on the vector of the fused feature. The statistics show that the accuracy of AML class is 100 percent, ALL reached the accuracy of 94.318 percent, and accuracy of MM is gained around 94.44 percent. Sensitivity, precision, F1-score etc are cited below in table 4.35. The confusion matrix on Serial fusion is shown in Figure-4-17.

Table 4.34: Statistics of Bagging Esembler using Serial Fusion

Class	Accuracy %	Sensitivity %	Specificity %	Precision %	False Positive Rate %	F1 Score %
ALL	94.318	94.318	97.253	94.318	2.7473	94.318
AML	100	100	100	100	0	100
MM	94.444	94.444	97.222	94.444	2.7778	94.444

Overall accuracy gained by Bagging Ensembler on ALL, AML and MM was 96.30 %. The overall statistics of Bagging Ensembler are given below in the table 4.36

Table 4.35: Overall Statistics of Bagging Esembler using Serial Fusion

Statistics	Results in %
Accuracy	96.30
Error	3.70
Sensitivity	96.25
Specificity	98.16
Precision	96.25
False Positive Rate	01.84
F1_score	96.25
Matthews Correlation Coefficient	94.41

Figure 4.17: Confusion Matrix of Bagging Esembler

Serial Fusion using Bag Essembler		
True Class	ALL	MM
	82	92
	6	84
ALL	93.2%	100.0%
AML	6.8%	6.7%
MM	93.3%	6.7%
Predicted Class		

4.6.8: Statistical Analysis of Coarse KNN on Serial Fusion

This section has discussed the reported statistics of the most famous traditional machine learning algorithm, Coarse KNN classifier, to classify the lesion on the vector of the fused feature. The statistics show that the accuracy of AML class is 100 percent, ALL reached the accuracy of 84.091 percent, and accuracy of MM is gained around 97.78 percent. Sensitivity, precision, F1-score etc are cited below in table 4.37. The confusion matrix on Serial fusion is shown in Figure-4-18.

Table 4.36: Statistics of Coarse KNN using Serial Fusion

Class	Accuracy %	Sensitivity %	Specificity %	Precision %	False Positive Rate %	F1 Score %
ALL	84.091	84.091	98.901	97.368	1.0989	90.244
AML	100	100	100	100	0	100
MM	97.778	97.778	92.222	86.275	7.7778	91.667

Overall accuracy gained by Coarse KNN on ALL, AML and MM was 93.95 %.

The overall statistics of Coarse KNN are given below in the table 4.38

Table 4.37: Overall Statistics of Coarse KNN using Serial Fusion

Statistics	Results in %
Accuracy	93.95
Error	5.93
Sensitivity	93.96
Specificity	97.04
Precision	94.55
False Positive Rate	02.96
F1_score	91.34
Matthews Correlation Coefficient	86.67

Figure 4.18: Confusion Matrix of Coarse KNN

Serial Fusion using Coarse KNN			
True Class	ALL	AML	MM
	74	92	88
	14	2	2
Predicted Class	ALL	AML	MM
84.1%	100.0%	97.8%	15.9%
15.9%		2.2%	
97.4%	100.0%	86.3%	
2.6%		13.7%	

4.7: Classification Results using PCA Fusion

After CCA and Serial Fusion, we also have analysed other technique of featured concatenation using PCA Fusion. The features extracted by CNN-1 and CNN-2 are also concatenated into a single enhanced vector through PCA Fusion. After that, the fused vectors of enhanced features were passed out to the classifiers to classify the input images. Bagging Ensemble, Total Boost Ensemble, Fine K-Nearest Neighbour (FK-NN), RUSBoost, LPBoost Coarse K-Nearest Neighbour (Coarse K-NN), and Support Vector Machine (SVM) are some of the classifiers; used in the proposed methodology. We have implemented multiple classifiers of machine learning in this step.

4.7.1: Statistical Analysis of SVM on PCA Fusion

This section has discussed the reported statistics of the most famous traditional machine learning algorithm, SVM classifier, to classify the lesion on the vector of the fused feature. The statistics show that the accuracy of AML class is 100 percent, ALL reached the accuracy of 90.909 percent, and accuracy of MM is gained around 95.556 percent. Sensitivity, precision, F1-score etc are cited below in table 4.38. The confusion matrix on PCA fusion is shown in Figure-4-19.

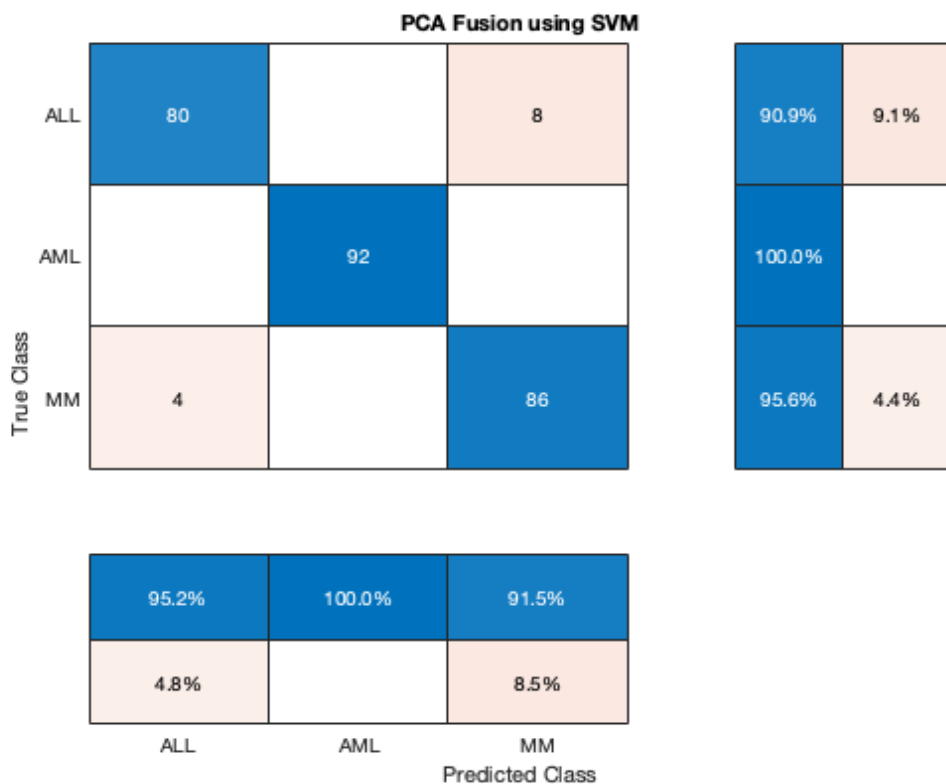
Table 4.38: Statistics of SVM using PCA Fusion

Class	Accuracy %	Sensitivity %	Specificity %	Precision %	False Positive Rate %	F1 Score %
ALL	90.909	90.909	97802	95238	2.1978	93023
AML	100	100	100	100	0	100
MM	95556	95556	95.556	91489	4.4444	93478

Overall accuracy gained by SVM on ALL, AML and MM was 95.56 %. The overall statistics of SVM are given below in the table 4.29

Table 4.39: Overall Statistics of SVM using PCA Fusion

Statistics	Results in %
Accuracy	95.56
Error	4.07
Sensitivity	9549
Specificity	97.79
Precision	9558
False Positive Rate	2.21
F1_score	95.50
Matthews Correlation Coefficient	93.93

Figure 4.19: Confusion Matrix of SVM

4.7.2: Statistical Analysis on Fine KNN PCA Fusion

This section has discussed the reported statistics of the most famous traditional machine learning algorithm, Fine KNN classifier, to classify the lesion on the vector of the fused feature. The statistics show that the accuracy of AML class is 96.703 percent, ALL reached the accuracy of 93.182 percent, and accuracy of MM is gained around 93.33 percent. Sensitivity, precision, F1-score etc are cited below in table 4.40. The confusion matrix on PCA fusion is shown in Figure-4-20.

Table 4.40: Statistics of Fine KNN using PCA Fusion

Class	Accuracy %	Sensitivity %	Specificity %	Precision %	False Positive Rate %	F1 Score %
ALL	93.182	93.182	96.703	93.182	2.1978	93.182
AML	100	100	100	100	0	100
MM	93.333	93.333	96.667	93.333	3.33	93.333

Overall accuracy gained by Fine KNN on ALL, AML and MM was 95.05%. The overall statistics of Fine KNN are given below in the table 4.41

Table 4.41: Overall Statistics of Fine KNN using PCA Fusion

Statistics	Results in %
Accuracy	95.05
Error	4.44
Sensitivity	95.51
Specificity	97.79
Precision	95.51
False Positive Rate	2.21
F1_score	95.51
Matthews Correlation Coefficient	90.00

Figure 4.20: Confusion Matrix of Fine KNN

PCA Fusion using Fine KNN			
True Class	ALL	ALL	
	AML	AML	
	MM	MM	
	82	6	93.2% 6.8%
	92		100.0%
	6	84	93.3% 6.7%
Predicted Class			
	93.2%	100.0%	93.3%
	6.8%		6.7%

4.7.3: Statistical Analysis of Medium KNN on PCA Fusion

This section has discussed the reported statistics of the most famous traditional machine learning algorithm, Medium KNN classifier, to classify the lesion on the vector of the fused feature. The statistics show that the accuracy of AML class is 100 percent, ALL reached the accuracy of 92.045 percent, and accuracy of MM is gained around 97.78 percent. Sensitivity, precision, F1-score etc are cited below in table 4.42. The confusion matrix on PCA fusion is shown in Figure-4-21.

Table 4.42: Statistics of Medium KNN using PCA Fusion

Class	Accuracy %	Sensitivity %	Specificity %	Precision %	False Positive Rate %	F1 Score %
ALL	92.045	92.045	98.901	97.59	1.0989	94.737
AML	100	100	100	100	0	100
MM	97.778	97.778	96.111	92.632	3.8889	95.135

Overall accuracy gained by Medium KNN on ALL, AML and MM was 96.67 %.

The overall statistics of Medium KNN are given below in the table 4.43

Table 4.43: Overall Statistics of Medium using PCA Fusion

Statistics	Results in %
Accuracy	96.67
Error	3.33
Sensitivity	96.61
Specificity	98.34
Precision	96.74
False Positive Rate	1.66
F1_score	96.62
Matthews Correlation Coefficient	95.02

Figure 4.21: Confusion Matrix of Medium KNN

PCA Fusion using Medium KNN		
True Class	ALL	MM
	81	92
	2	88
ALL	97.6%	100.0%
AML	2.4%	
MM		92.6%
Predicted Class		

4.7.4: Statistical Analysis of RUSBoost on PCA Fusion

This section has discussed the reported statistics of the most famous traditional machine learning algorithm, RUSBoost classifier, to classify the lesion on the vector of the fused feature. The statistics show that the accuracy of AML class is 100 percent, ALL reached the accuracy of 94.318 percent, and accuracy of MM is gained around 95.56 percent. Sensitivity, precision, F1-score etc are cited below in table 4.44. The confusion matrix on PCA fusion is shown in Figure-4-22.

Table 4.44: Statistics of RUSBoost using PCA Fusion

Class	Accuracy %	Sensitivity %	Specificity %	Precision %	False Positive Rate %	F1 Score %
ALL	94.318	94.318	97.802	95.402	2.1978	94.857
AML	100	100	100	100	0	100
MM	95.556	95.556	97.222	94.505	2.7778	95.028

Overall accuracy gained by RUSBoost on ALL, AML and MM was 96.67%. The overall statistics of RUSBoost are given below in the table 4.45.

Table 4.45: Overall Statistics of RUSBoost using PCA Fusion

Statistics	Results in %
Accuracy	96.67
Error	3.33
Sensitivity	96.62
Specificity	98.34
Precision	96.64
False Positive Rate	1.66
F1_score	96.63
Matthews Correlation Coefficient	94.97

Figure 4.22: Confusion Matrix of RUSBoost

PCA Fusion using RUSBoost			
True Class	ALL	ALL	
	AML	AML	
	MM	MM	
	83	5	94.3% 5.7%
	92		100.0%
	4	86	95.6% 4.4%
	95.4%	100.0%	94.5%
	4.6%		5.5%
Predicted Class			

4.7.5: Statistical Analysis of TotalBoost on PCA Fusion

This section has discussed the reported statistics of the most famous traditional machine learning algorithm, TotalBoost classifier, to classify the lesion on the vector of the fused feature. The statistics show that the accuracy of AML class is 100 percent, ALL reached the accuracy of 94.318 percent, and accuracy of MM is gained around 96.667 percent. Sensitivity, precision, F1-score etc are cited below in table 4.46. The confusion matrix on PCA fusion is shown in Figure-4-23.

Table 4.46: Statistics of TotalBoost using PCA Fusion

Class	Accuracy %	Sensitivity %	Specificity %	Precision %	False Positive Rate %	F1 Score %
ALL	94.318	94.318	98.352	96.512	1.6484	95.402
AML	100	100	100	100	0	100
MM	96.667	96.667	97.222	94.565	2.7778	95.604

Overall accuracy gained by TotalBoost on ALL, AML and MM was 96.95 %. The overall statistics of TotalBoost are given below in the table 4.47

Table 4.47: Overall Statistics of TotalBoost using PCA Fusion

Statistics	Results in %
Accuracy	96.95
Error	3.05
Sensitivity	95.49
Specificity	98.52
Precision	97.03
False Positive Rate	1.48
F1_score	97.00
Matthews Correlation Coefficient	95.54

Figure 4.23: Confusion Matrix of Total Boost

PCA Fusion using TotalBoost			
True Class	ALL	MM	
	ALL	83	5
	MM	4	86
Predicted Class			
ALL	95.4%	100.0%	94.5%
MM	4.6%		5.5%

4.7.6: Statistical Analysis of LPBoost on PCA Fusion

This section has discussed the reported statistics of the most famous traditional machine learning algorithm, LPBoost classifier, to classify the lesion on the vector of the fused feature. The statistics show that the accuracy of AML class is 100 percent, ALL reached the accuracy of 94.318 percent, and accuracy of MM is gained around 93.333 percent. Sensitivity, precision, F1-score etc are cited below in table 4.48. The confusion matrix on PCA fusion is shown in Figure-4-24.

Table 4.48: Statistics of LPBoost using PCA Fusion

Class	Accuracy %	Sensitivity %	Specificity %	Precision %	False Positive Rate %	F1 Score %
ALL	94.318	94.318	96.703	93.258	3.2967	93.785
AML	100	100	100	100	0	100
MM	93.333	93.333	97.222	94.382	2.7778	93.855

Overall accuracy gained by LPBoost on ALL, AML and MM was 96.67 %. The overall statistics of LPBoost are given below in the table 4.49

Table 4.49: Overall Statistics of LPBoost using PCA Fusion

Statistics	Results in %
Accuracy	96.67
Error	3.33
Sensitivity	96.62
Specificity	98.34
Precision	96.64
False Positive Rate	1.66
F1_score	96.63
Matthews Correlation Coefficient	94.97

Figure 4.24: Confusion Matrix of LPBoost

PCA Fusion using LPBoost			
True Class	ALL	MM	
	ALL	82	6
	MM	4	86
Predicted Class			
ALL	95.3%	100.0%	93.5%
AML	4.7%		6.5%

4.7.7: Statistical Analysis of Bagging Ensembler on PCA Fusion

This section has discussed the reported statistics of the most famous traditional machine learning algorithm, Bagging Ensembler classifier, to classify the lesion on the vector of the fused feature. The statistics show that the accuracy of AML class is 100 percent, ALL reached the accuracy of 93.182 percent, and accuracy of MM is gained around 95.556 percent. Sensitivity, precision, F1-score etc are cited below in table 4.50. The confusion matrix on PCA fusion is shown in Figure-4-25

Table 4.50: Statistics of Bagging Esembler using PCA Fusion

Class	Accuracy %	Sensitivity %	Specificity %	Precision %	False Positive Rate %	F1 Score %
ALL	93.182	93.182	97.802	95.349	2.1978	94.253
AML	100	100	100	100	0	100
MM	95.556	95.556	96.667	93.478	3.333	94.505

Overall accuracy gained by Bagging Ensembler on ALL, AML and MM was 96.30 %. The overall statistics of Bagging Ensembler are given below in the table 4.51

Table 4.51: Overall Statistics of Bagging Esembler using PCA Fusion

Statistics	Results in %
Accuracy	96.30
Error	3.70
Sensitivity	96.25
Specificity	98.16
Precision	96.25
False Positive Rate	01.84
F1_score	96.25
Matthews Correlation Coefficient	94.42

Figure 4.25: Confusion Matrix of Bagging Esembler

PCA Fusion using Bagging Ensembler			
True Class	ALL	AML	MM
	82	92	86
	6		
	93.2%	100.0%	95.6%
	6.8%		4.4%
Predicted Class			
ALL	95.3%	100.0%	93.5%
AML	4.7%		6.5%

4.7.8: Statistical Analysis of Coarse KNN on PCA Fusion

This section has discussed the reported statistics of the most famous traditional machine learning algorithm, Coarse KNN classifier, to classify the lesion on the vector of the fused feature. The statistics show that the accuracy of AML class is 100 percent, ALL reached the accuracy of 84.364 percent, and accuracy of MM is gained around 97.78 percent. Sensitivity, precision, F1-score etc are cited below in table 4.52. The confusion matrix on PCA fusion is shown in Figure-4-26.

Table 4.52: Statistics of Coarse KNN using PCA Fusion

Class	Accuracy %	Sensitivity %	Specificity %	Precision %	False Positive Rate %	F1 Score %
ALL	86.364	86.364	99.451	98.701	0.54945	92.121
AML	100	96.739	100	100	0	98.343
MM	97.778	97.778	92.222	86.275	8.3333	91.667

Overall accuracy gained by Coarse KNN on ALL, AML and MM was 93.99 %.

The overall statistics of Coarse KNN are given below in the table 4.53

Table 4.53: Overall Statistics of Coarse KNN using PCA Fusion

Statistics	Results in %
Accuracy	93.99
Error	5.93
Sensitivity	94.00
Specificity	97.04
Precision	94.76
False Positive Rate	2.96
F1_score	94.07
Matthews Correlation Coefficient	91.45

Figure 4.26: Confusion Matrix of Coarse KNN

PCA Fusion using Coarse KNN			
True Class	ALL	MM	
	ALL	89	12
	MM	1	89
Predicted Class			
	ALL	AML	MM
98.7%	100.0%	85.6%	
1.3%			14.4%

4.8: Discussion and Comparison

In this section, we will be discussing the results of our proposed methodology with the past work. After acquisition of images, we performed pre-processing, which was used to enhance the image quality, removed noise and sharpen of image dataset. Moreover, in pre-processing we have also achieved the segmentation. No special model was trained to segment the image dataset. Segmentation itself has been performed in pre-processing, thus this helps us in less computation to get image dataset segmented but also has reduced time of computation. In next step, we trained two models of CNN that works parallel to extract features from dataset. After performing activation on extracted vectors of feature, which was the output of each CNNs, we performed CCA fusion to extract and concatenate the most promising featured vector, which is also our contribution. We also have compared CCA fusion with Principal Component Analysis (PCA) and Serial Based Approach SBA. Lastly, we use traditional machine learning models to train and test. The reason for using machine learning traditional model was to minimise the computation of our network. Traditional machine learning models take few minutes to get trained but if we use deep learning network in this step, it might take several hours or even few days. By using traditional machine learning algorithms, we observed that the best one on our proposed was Bagging ensemble model which gives us accuracy of 97.04 percent overall. But SVM and Coarse KNN gives us worst result among used classifiers in our proposed methodology. The accuracy observed by both SVM and Coarse KNN was around 95%, which is not even so bad at all.

Furthermore, comparison between CCA, PCA, and SBA was also performed to validate the comparative analysis between them. According to the experimental results performed on CCA, PCA, and SBA, we had concluded that CCA produced the best results compared to feature concatenation techniques with an accuracy of 97.04% with the Bagging Ensemble Model. The statistics of CCA, PCA, and SBA on traditional machine learning models are listed below in the table 4.19.

Table-4.54: Comparison of CCA, SBA, and PCA on ML Models

Accuracy of ML Models	CCA Results %	SBA Results %	PCA Results %
Bagging Boost	97.04	96.30	96.25
Coarse KNN	95.19	93.95	93.99
Fine KNN	95.93	96.25	95.50
LPBoost	96.30	96.67	95.93
Medium KNN	96.30	95.93	96.67

RUSBoost	95.56	94.07	96.67
SVM	95.19	95.93	95.56

At the end, we are going to discuss the statistics of our proposed methodology with the previous work. Our proposed methodology has improved the results significantly, the results are cited below in the table.

Table-4.55: Comparison of Proposed Methodology

Author/Year	Methodology	Disease	Statistics
(Bodzas et al., 2020)	ANN & SVM	Acute Lymphoblastic Leukaemia (ALL)	Specificity: 95.31%
(Di Ruberto et al., 2020)	CNN & SVM	leukaemia	94.1%
(Hegde et al., 2019)	Active Contours	Leukocytes	96.5%
(Shree & Janani, 2019)	Alexnet	Leukocytes	90.30

CHAPTER-05

CONCLUSION

Leukaemia is a form of blood cancer that occurs when the bone marrow of our bodies produces an abundance of white blood cells. This illness not only affects humans but's also widespread cancer in children. Treatment for leukaemia is determined by the form of cancer and how far it has spread across the body. It is essential to detect this disorder as soon as possible to get appropriate treatment and recover. The research developed an automated diagnosis tool for acute lymphoblastic leukaemia (ALL), acute myeloid leukaemia (AML), and multiple myeloma using a convolutional neural network (CNN) model (MM). Using microscopic blood smear images, the model detects malignant leukaemia cells. The dataset was pre-processed using our recommended methodology to minimise noise, blurriness and enhance image quality. During pre-processing, we found that the output images had already been segmented. The approach is practical and does not necessitate image segmentation. Following that, we trained two CCN models in parallel to extract features. The CCA Fused approach is used to concatenate these derived features. The classifier receives lastly fused vectors (SVM, Bagging ensemble, total boost, RUSBoost, Fine KNN etc.). Using the Bagging ensemble design, we were able to achieve a 97.04 percent accuracy. As a result, pathologists may find that this procedure aids in effective diagnosis.

REFERENCES

- Abdeldaim, A. M., Sahlol, A. T., Elhoseny, M., & Hassanien, A. E. (2018). Computer-aided acute lymphoblastic leukemia diagnosis system based on image analysis. *Advances in Soft Computing and Machine Learning in Image Processing*, 131–147.
- Agaian, S., Madhukar, M., & Chronopoulos, A. T. (2014). Automated Screening System for Acute Myelogenous Leukemia Detection in Blood Microscopic Images. *IEEE Systems Journal*, 8(3).
- Al-Tahhan, F. E., Sakr, A. A., Aladle, D. A., & Fares, M. E. (2019). Improved image segmentation algorithms for detecting types of acute lymphatic leukaemia. *IET Image Processing*, 13(13), 2595–2603.
- Ali, H., Sharif, M., Yasmin, M., Husain, M., & Farhan, R. (2019). A survey of feature extraction and fusion of deep learning for detection of abnormalities in video endoscopy of gastrointestinal-tract. *Artificial Intelligence Review*. <https://doi.org/10.1007/s10462-019-09743-2>
- Alsalem, M. A., Zaidan, A. A., Zaidan, B. B., Albahri, O. S., Alamoodi, A. H., Albahri, A. S., Mohsin, A. H., & Mohammed, K. I. (2019). Multiclass Benchmarking Framework for Automated Acute Leukaemia Detection and Classification Based on BWM and Group-VIKOR. *Journal of Medical Systems*, 43(7), 212. <https://doi.org/10.1007/s10916-019-1338-x>
- Anwar, S., & Alam, A. (2020). A convolutional neural network-based learning approach to acute lymphoblastic leukaemia detection with automated feature extraction. *Medical & Biological Engineering & Computing*, 58(12), 3113–3121.
- Bagasjvara, R. G., Candradewi, I., Hartati, S., & Harjoko, A. (2016). Automated detection and classification techniques of Acute leukemia using image processing: A review. *2016 2nd International Conference on Science and Technology-Computer (ICST)*, 35–43. <https://doi.org/10.1109/ICSTC.2016.7877344>
- Basima, C. T., & Panicker, J. R. (2016). Enhanced leucocyte classification for leukaemia detection. *2016 International Conference on Information Science (ICIS)*, 65–71. <https://doi.org/10.1109/INFOSCI.2016.7845302>
- Bhattacharjee, R., & Saini, L. M. (2015). Robust technique for the detection of Acute Lymphoblastic Leukemia. *2015 IEEE Power, Communication and Information Technology Conference (PCITC)*, 657–662. <https://doi.org/10.1109/PCITC.2015.7438079>
- Bodzas, A., Kodytek, P., & Zidek, J. (2020). Automated detection of acute lymphoblastic leukemia from microscopic images based on human visual perception. *Frontiers in Bioengineering and Biotechnology*, 8, 1005.
- Brownlee, J. (2019). *Transfer Learning in Keras with Computer Vision Models*. Machine Learning Mastery.
- Chen, J., Narayanan, S., Collins, D., Smith, S., Matthews, P., & Arnold, D. (2004). Relating neocortical pathology to disability progression in multiple sclerosis using MRI. *23(3)*, 1168–1175.
- Clark, K., Vendt, B., Smith, K., Freymann, J., Kirby, J., Koppel, P., Moore, S., Phillips, S., Maffitt, D., Pringle, M., Tarbox, L., & Prior, F. (2013). The Cancer Imaging Archive (TCIA): Maintaining and Operating a Public Information Repository. *Journal of Digital Imaging*, 26(6), 1045–1057. <https://doi.org/10.1007/s10278-013-9622-7>
- Contributors, W. (2019). *Blood*. Wikipedia, The Free Encyclopedia. <https://doi.org/905460149>
- Dharani, T., & Hariprasath, S. (2018). Diagnosis of Leukemia and its types Using Digital Image Processing Techniques. *2018 3rd International Conference on Communication and Electronics Systems (ICCES)*, 275–279.
- Di Ruberto, C., Loddo, A., & Puglisi, G. (2020). Blob Detection and Deep Learning for Leukemic Blood Image Analysis. *Applied Sciences*, 10(3), 1176.
- Goutam, D., & Sailaja, S. (2015). Classification of acute myelogenous leukemia in blood microscopic images using supervised classifier. *IEEE International Conference on Engineering and Technology (ICETECH)*, 1–5.

- https://doi.org/10.1109/ICETECH.2015.7275021
- Gupta, A., Duggal, R., Gehlot, S., Gupta, R., Mangal, A., Kumar, L., Thakkar, N., & Satpathy, D. (2020). GCTI-SN: Geometry-inspired chemical and tissue invariant stain normalization of microscopic medical images. *Medical Image Analysis*, 65, 101788. https://doi.org/https://doi.org/10.1016/j.media.2020.101788
- Gupta, A., Mallick, P., Sharma, O., Gupta, R., & Duggal, R. (2018). PCSeg: Color model driven probabilistic multiphase level set based tool for plasma cell segmentation in multiple myeloma. *PLOS ONE*, 13(12), e0207908. https://doi.org/10.1371/journal.pone.0207908
- Haghigiat, M., Abdel-Mottaleb, M., & Alhalabi, W. (2016). Fully automatic face normalization and single sample face recognition in unconstrained environments. *Expert Systems with Applications*, 47, 23–34. https://doi.org/https://doi.org/10.1016/j.eswa.2015.10.047
- Hegde, R. B., Prasad, K., Hebbar, H., & Singh, B. M. K. (2019). Image Processing Approach for Detection of Leukocytes in Peripheral Blood Smears. *Journal of Medical Systems*, 43(5), 114. https://doi.org/10.1007/s10916-019-1219-3
- Jagadev, P., & Virani, H. G. (2017). Detection of leukemia and its types using image processing and machine learning. *2017 International Conference on Trends in Electronics and Informatics (ICEI)*, 522–526. https://doi.org/10.1109/ICOEI.2017.8300983
- Kassani, S. H., & Kassani, P. H. (2019). A comparative study of deep learning architectures on melanoma detection. *Tissue and Cell*, 58, 76–83.
- Kassani, S. H., Wesolowski, M. J., Schneider, K. A., & Deters, R. (2019). A Hybrid Deep Learning Architecture for Leukemic B-lymphoblast Classification. *ArXiv Preprint ArXiv:1909.11866*.
- Matek, C., Schwarz, S., Spiekermann, K., & Marr, C. (2019). Human-level recognition of blast cells in acute myeloid leukaemia with convolutional neural networks. *Nature Machine Intelligence*, 1(11), 538–544.
- Mishra, S., Sharma, L., Majhi, B., & Sa, P. K. (2017). *Microscopic Image Classification Using DCT for the Detection of Acute Lymphoblastic Leukemia (ALL)*. 171–180.
- Mohajerani, P., & Ntziachristos, V. (2019). Classification of Normal Versus Malignant Cells in B-ALL Microscopic Images Based on a Tiled Convolution Neural Network Approach. In A. Gupta & R. Gupta (Eds.), *ISBI 2019 C-NMC Challenge: Classification in Cancer Cell Imaging* (pp. 103–111). Springer Singapore.
- Natasha Honomichl. (2019a). *MiMM_SBILab Dataset: Microscopic Images of Multiple Myeloma*. Wiki Cancer Image Archive.
- Natasha Honomichl. (2019b). *SN-AM Dataset: White Blood cancer dataset of B-ALL and MM for stain normalization*. Wiki Cancer Image Archive.
- Organization, W. H. (2020). *Cancer Tomorrow*. International Agency for Research on Cancer.
- Patel, N., & Mishra, A. (2015). Automated Leukaemia Detection Using Microscopic Images. *Procedia Computer Science*, 58, 635–642. https://doi.org/https://doi.org/10.1016/j.procs.2015.08.082
- Pham, T.-C., Luong, C.-M., Visani, M., & Hoang, V.-D. (2018). Deep CNN and data augmentation for skin lesion classification. *Asian Conference on Intelligent Information and Database Systems*, 573–582.
- Rawat, J., Singh, A., Bhaduria, H. S., & Virmani, J. (2015). Computer aided diagnostic system for detection of leukemia using microscopic images. *Procedia Computer Science*, 70, 748–756.
- Rawat, J., Singh, A., Bhaduria, H. S., Virmani, J., & Devgun, J. S. (2017). Classification of acute lymphoblastic leukaemia using hybrid hierarchical classifiers. *Multimedia Tools and Applications*, 76(18), 19057–19085. https://doi.org/10.1007/s11042-017-4478-3
- Rawat, J., Singh, A., Hs, B., Virmani, J., & Devgun, J. S. (2017). Computer assisted classification framework for prediction of acute lymphoblastic and acute myeloblastic leukemia. *Biocybernetics and Biomedical Engineering*, 37(4), 637–654. https://doi.org/https://doi.org/10.1016/j.bbe.2017.07.003
- Rehman, A., Abbas, N., Saba, T., Rahman, S. I. ur, Mehmood, Z., & Kolivand, H. (2018). Classification of acute lymphoblastic leukemia using deep learning. *Microscopy Research and Technique*, 81(11), 1310–1317. https://doi.org/10.1002/jemt.23139

- Shah, S., Nawaz, W., Jalil, B., & Khan, H. A. (2019). Classification of Normal and Leukemic Blast Cells in B-ALL Cancer Using a Combination of Convolutional and Recurrent Neural Networks. In A. Gupta & R. Gupta (Eds.), *ISBI 2019 C-NMC Challenge: Classification in Cancer Cell Imaging* (pp. 23–31). Springer Singapore.
- Shree, K. D., & Janani, B. (2019). Classification of Leucocytes for Leukaemia Detection. *Research Journal of Engineering and Technology*, 10(2), 59–66.
- Society, A. C. (2019). *Key Statistics for Leukemia*. American Cancer Society. <https://cancerstatisticscenter.cancer.org/#!/cancer-site/Leukemia>
- Subrajeet, M., Dipti, P., Satpathi, & Sanghamitra. (n.d.). *Image Analysis of Blood Microscopic Images for Acute Leukemia Detection*.
- Sukhia, K. N., Ghafoor, A., Riaz, M. M., & Iltaf, N. (2019). Automated acute lymphoblastic leukaemia detection system using microscopic images. *IET Image Processing*, 13(13), 2548–2553.
- Sun, Q.-S., Zeng, S.-G., Heng, P.-A., & Xia, D.-S. (2004). Feature fusion method based on canonical correlation analysis and handwritten character recognition. *ICARCV 2004 8th Control, Automation, Robotics and Vision Conference, 2004.*, 2, 1547–1552 Vol. 2. <https://doi.org/10.1109/ICARCV.2004.1469081>
- Tajbakhsh, N., Shin, J. Y., Gurudu, S. R., Hurst, R. T., Kendall, C. B., Gotway, M. B., & Liang, J. (2016). Convolutional neural networks for medical image analysis: Full training or fine tuning? *IEEE Transactions on Medical Imaging*, 35(5), 1299–1312.
- Vaghela, H. P., Modi, H., Pandya, M., & Potdar, M. B. (2015). Leukemia detection using digital image processing techniques. *Leukemia*, 10(1), 43–51.
- Vincent, I., Kwon, K., Lee, S., & Moon, K. (2015). Acute lymphoid leukemia classification using two-step neural network classifier. *2015 21st Korea-Japan Joint Workshop on Frontiers of Computer Vision (FCV)*, 1–4. <https://doi.org/10.1109/FCV.2015.7103739>
- Vogado, L. H. S., de MS Veras, R., Andrade, A. R., e Silva, R. R. V., de Araujo, F. H. D., & de Medeiros, F. N. S. (2016). Unsupervised leukemia cells segmentation based on multi-space color channels. *2016 IEEE International Symposium on Multimedia (ISM)*, 451–456.
- Vogado, L. H. S., Veras, R. M. S., Araujo, F. H. D., Silva, R. R. V., & Aires, K. R. T. (2018). Leukemia diagnosis in blood slides using transfer learning in CNNs and SVM for classification. *Engineering Applications of Artificial Intelligence*, 72, 415–422. <https://doi.org/https://doi.org/10.1016/j.engappai.2018.04.024>
- World Health Organization. (2019). *International Agency for Research on Cancer*. World Health Organization. <https://gco.iarc.fr/today/data/factsheets/populations/586-pakistan-fact-sheets.pdf>
- Zhao, J., Zhang, M., Zhou, Z., Chu, J., & Cao, F. (2017). Automatic detection and classification of leukocytes using convolutional neural networks. *Medical & Biological Engineering & Computing*, 55(8), 1287–1301. <https://doi.org/10.1007/s11517-016-1590-x>

APPENDIX-01

Abbreviation Used in the Thesis		
Sr#	Item	Abbreviation
1	Artificial Neural Networks	ANN
2	Back-Propagation Neural Networks	BPNN
3	Conventional Neural Networks	CNN
4	Naive Bayes Gaussian	NB-G
5	Naive Bayes Kernel Data Distribution	NB-K
6	Random Forest Algorithm	RFM
7	Simple Threshold Method	STM
8	Support Vector Machine	SVM
9	Support Vector Machine Proximal	SVM-P
10	Support Vector Machine Radial Basis Function	SVM-RBF
11	Three Normalisation Technique	3-N

APPENDIX-02

Turnitin Originality Report

Tested on 11-August-2021 by Turnitin Anti Plagiarism Software Provided by Higher Education Commission, Pakistan to the Instructors of the University of Gujrat, Pakistan.

Thesis Title: "A Novel Deep Learning Framework for the Detection of Lymphocytes Cancer and its Types"

Author Name: Raheel Baig

Institution: University of Gujrat, Pakistan

PRIMARY SOURCES

SIMILARITY INDEX	INTERNET SOURCES	PUBLICATIONS	STUDENT PAPERS
6 %	5 %	2 %	1 %
Internet Source			
<hr/>			
1.	bmcgenomics.biomedcentral.com		
2.	worldwidescience.org		
3.	biomedical-engineering-online.biomedcentral.com		
4.	sbilab.iiitd.edu.in		
5.	theses.gla.ac.uk		
6.	wiki.cancerimagingarchive.net		5%
7.	cps-vo.org		
8.	pure.uva.nl		
9.	trid.trb.org		
10.	seer.cancer.gov		
11.	prod--journal.elife sciences.org		
12.	repozitorij.svkst.unist.hr		
<hr/>			
Publication			
<hr/>			
1.	Saban Ozturk, Umut Ozkaya, Bayram Akdemir, Levent Seyfi. "Convolution Kernel Size Effect on Convolutional Neural Network in Histopathological Image Processing Applications", 2018 International Symposium on Fundamentals of Electrical Engineering (ISFEE), 2018		
2.	"Malware Analysis Using Artificial Intelligence and Deep Learning", Springer Science and Business Media LLC, 2021		2%
3.	"Intelligent Computing Theories and Application", Springer Science and Business Media LLC, 2019		
4.	F.E. Al Tahhan, Ali A. Sakr, Doaa A. Aladle, M.E. Fares. "Improved image segmentation algorithms for detecting types of acute lymphatic leukaemia", IET Image Processing, 2019		

-
- - 5. Deepika Kumar, Nikita Jain, Aayush Khurana, Sweta Mittal, Suresh Chandra Satapathy, Roman Senkerik, Jude D. Hemanth. "Automatic Detection of White Blood Cancer From Bone Marrow Microscopic Images Using Convolutional Neural Networks", IEEE Access, 2020
 - 6. M. MÜLLER-PREMURU, P. ČERNELČ. "Molecular epidemiology of catheter-related bloodstream infections caused by coagulase-negative staphylococci in haematological patients with neutropenia", Epidemiology and Infection, 2004
 - 7. Huseyin Duysak, Umut Ozkaya, Enes Yigit."Determination of the Amount of Grain in Silos with Deep Learning Methods Based on Radar Spectrogram Data", IEEE Transactions on Instrumentation and Measurement, 2021
 - 8. Jan Kuschan, Moritz Burgdorff, Hristo Filaretov, Jörg Krüger. "Inertial Measurement Unit based Human Action Recognition for Soft-Robotic Exoskeleton", IOP Conference Series: Materials Science and Engineering, 2021
 - 9. "Proceedings of the 1st International Conference on Smart Innovation, Ergonomics and Applied Human Factors (SEAHF)", Springer Science and Business Media LLC, 2019

Student Paper

- 1. Submitted to October University for Modern Sciences and Arts (MSA) 1%
 - 2. Submitted to Asian Institute of Technology
-